The Flow Goes Ever On: An Introduction to Complex Fluids

Boulder Summer School Lectures
Saverio E. Spagnolie

September 30, 2026

Contents

1 Introduction **1**
1.1 The effective stress tensor . . . 2
1.2 The Newtonian approximation . . . 2
1.3 Notation and conventions . . . 2
1.4 Further reading . . . 3

2 Lecture 1: From Batchelor's formula to Einstein's effective viscosity **4**
2.1 Reduction to a surface integral: the stresslet . . . 4
2.2 The disturbance flow due to a single spherical particle . . . 6
2.3 The singularity method for Stokes flow (Green's functions) . . . 7
2.4 Computing the surface traction, and the extra particle stress . . . 9

3 Lecture 2: Kinetic theory and suspensions of rods **11**
3.1 Particle distribution function and the continuity equation . . . 11
3.2 Slender body theory and orientational dynamics . . . 13
3.3 Computing the extra particle stress . . . 15
3.4 Equilibrium distributions with no flow: Boltzmann to Bingham . . . 16
3.5 Suspension rheology and shear thinning . . . 17
3.6 The closure problem . . . 18
3.7 The Carreau-Yasuda and power-law models . . . 20

4 Lecture 3: From Hookean Dumbbells to Oldroyd-B and Active Suspensions **21**
4.1 From rods to Hookean dumbbells . . . 22
4.2 Health warning: the linear Maxwell model is not objective . . . 24
4.3 Active particles . . . 24
4.4 Active suspensions in complex fluids . . . 24

1 Introduction

In these notes I will introduce a number of key concepts in the continuum mechanics of complex fluids. A few classical non-Newtonian phenomena will be covered, including shear-dependent viscosity, viscoelasticity, and anisotropy. We will confine our attention to *dilute suspensions* of particles (small concentrations, well-separated bodies), be they passive or active, in a viscous solvent (e.g. water).

1.1 The effective stress tensor

The unifying object throughout is the *effective stress tensor* of the suspension,

$$\boldsymbol{\sigma}_{\text{eff}} = -p\,\mathbf{I} + \boldsymbol{\tau}, \tag{1.1}$$

where p is the pressure[1], and $\boldsymbol{\tau}$ is the 'deviatoric' stress. In a fluid which is host to a dilute suspension of particles, the viscous solvent plays a large role, and we further decompose the deviatoric stress as

$$\boldsymbol{\tau} = 2\mu\,\mathbf{E} + \boldsymbol{\Sigma}, \tag{1.2}$$

where μ is the solvent viscosity, $\mathbf{E} = \frac{1}{2}(\nabla\boldsymbol{u} + \nabla\boldsymbol{u}^T)$ is the rate-of-strain tensor, $\boldsymbol{u}$ is the velocity field, and $\boldsymbol{\Sigma}$ is the extra stress contributed by the particles. The first term is the standard Newtonian viscous stress. In general, $\boldsymbol{\Sigma}$ depends on the instantaneous positions, configurations, and activity of the immersed particles. But in a continuum approximation we will tend to average out many of those details, as we shall see.

Once we have found the extra stress, the Cauchy momentum equation (with no body force) takes the form:

$$\rho\frac{\mathrm{D}\boldsymbol{u}}{\mathrm{D}t} = \nabla\cdot\boldsymbol{\sigma} = -\nabla p + \mu\nabla^2\boldsymbol{u} + \nabla\cdot\boldsymbol{\Sigma}, \tag{1.3}$$

where $\mathrm{D}/\mathrm{D}t = \partial/\partial t + \boldsymbol{u}\cdot\nabla$ is the material derivative. The traction on any bounding surface (or large immersed body), with unit normal $\boldsymbol{\nu}$ pointing into the fluid, is given by $\boldsymbol{f} = \boldsymbol{\nu}\cdot\boldsymbol{\sigma} = -p\boldsymbol{\nu} + \boldsymbol{\nu}\cdot(2\mu\mathbf{E} + \boldsymbol{\Sigma})$. In the zero Reynolds number[2] limit, $\rho\,\mathrm{D}\boldsymbol{u}/\mathrm{D}t$ is vanishingly small when compared to the viscous damping on the right hand side, and is replaced by zero.

1.2 The Newtonian approximation

The Newtonian approximation is one in which the fluid stress is assumed to be linear in the instantaneous velocity gradient: $\boldsymbol{\sigma} = \mathcal{C} : \nabla\boldsymbol{u}$, or $\sigma_{ij} = \mathcal{C}_{ijk\ell}\partial_k u_\ell$, for some fourth-order tensor $\mathcal{C}$ (see below for relevant notation and conventions). In three dimensions there are then 81 different coefficients needed to characterize the fluid! But if the fluid is isotropic (its response to stress is independent of its orientation), and if the stress tensor is symmetric (more on this later) then only two coefficients survive: the only possibility is that $\boldsymbol{\sigma} = 2\mu\mathbf{E} + \lambda(\nabla\cdot\boldsymbol{u})\mathbf{I}$, where μ and λ are material constants, and $\mathbf{I}$ is the identity operator. This isotropic part is generally lumped into the pressure, or is just taken to be zero if the fluid is assumed to be incompressible.

A *quasi-Newtonian* fluid is one for which the stress tensor is still a constant times the local rate-of-strain tensor. This means that the extra stress must take the simple form $\boldsymbol{\Sigma} = 2\mu'\mathbf{E}$, for some added viscosity μ'. We will see a famous example of such a fluid in Lecture 1.

1.3 Notation and conventions

We use the index convention $(\nabla\boldsymbol{u})_{ij} = \partial_i u_j$, so that $\nabla := \partial/\partial\boldsymbol{x}$ (the "del" or "nabla" - harp!) operator behaves as a vector. A regular series expansion[3] of the jth component of the velocity field about a point $\boldsymbol{x} = \boldsymbol{X}$ is written as

$$u_j(\boldsymbol{x}) = u_j(\boldsymbol{X}) + (x-X)_i\partial_i u_j(\boldsymbol{X}) + \frac{1}{2}(x-X)_i(x-X)_k\partial_i\partial_k u_j(\boldsymbol{X}) + \ldots, \tag{1.4}$$

[1]The pressure, p, is often best viewed as a Lagrange multiplier which enforces incompressibility. We will often absorb isotropic components of complex fluid stresses into p, which does not affect the fluid flow.

[2]The Reynolds number, $\mathrm{Re} = \rho UL/\mu$, where ρ is the fluid density, and U and L are characteristic velocity and length scales, respectively, tends to be extremely small in the many biological systems of interest at the micron scale. But there are plenty of systems where complex fluid stresses are important in inertial settings. For example, oil companies add polymers to oil to reduce fluid drag along the walls in turbulent pipe flows.

[3]Health warning: we do a lot of Taylor expansion in this business, which assumes sufficient smoothness. Viscosity goes a long way towards providing such smoothness, but complex fluid stresses can in some cases result in discontinuous jumps in the velocity field. In such settings, expansions like this one need to be revisited.

where $\partial_i = \partial/\partial x_i$, and we are using the Einstein summation notation, where a repeated index in a product implies summation (for example, $\boldsymbol{x} \cdot \boldsymbol{u} = x_j u_j$). Returning to vector notation, the expansion above is then given by

$$\boldsymbol{u}(\boldsymbol{x}) = \boldsymbol{u}(\boldsymbol{X}) + (\boldsymbol{x} - \boldsymbol{X}) \cdot \nabla \boldsymbol{u}(\boldsymbol{X}) + \frac{1}{2}(\boldsymbol{x} - \boldsymbol{X})(\boldsymbol{x} - \boldsymbol{X}) : \nabla\nabla \boldsymbol{u}(\boldsymbol{X}) + ..., \tag{1.5}$$

where $\boldsymbol{x}\boldsymbol{x}$ and similar terms are dyadic products, and $\mathbf{A} : \mathbf{B} = \overline{A_{ij}} B_{ij}$ is the double dot product. This last convention is chosen so that $\mathbf{A} : \mathbf{A} = \mathrm{tr}(\mathbf{A}^H \mathbf{A}) \geq 0$, a sensible requirement for an inner product, so that it induces a norm. (Which norm? The Frobenius norm, $\|\mathbf{A}\|_F := (\mathbf{A} : \mathbf{A})^{1/2}$. The double dot product $\mathbf{A} : \mathbf{B}$ is also called the Frobenius inner product.) We can ignore the complex variables bits when the tensors are symmetric, as is the case in the example above, and will be the case for the rest of these notes.

We will spend a lot of time with the gradient of the velocity field, which we will decompose into its symmetric and antisymmetric parts,

$$\nabla \boldsymbol{u} = \mathbf{E} + \mathbf{W}, \tag{1.6}$$

where $\mathbf{E} = (\nabla \boldsymbol{u} + \nabla \boldsymbol{u}^T)/2$ and $\mathbf{W} = (\nabla \boldsymbol{u} - \nabla \boldsymbol{u}^T)/2$, or $W_{ij} = (\partial_i u_j - \partial_j u_i)/2$, and the vorticity is defined by $\boldsymbol{\omega} := \nabla \times \boldsymbol{u}$. If $\nabla \boldsymbol{u}$ does not vary in space, then we have that $\boldsymbol{r} \cdot \mathbf{W}^\infty = \frac{1}{2}\boldsymbol{\omega}^\infty \times \boldsymbol{r}$ for any vector $\boldsymbol{r}$.

1.4 Further reading

For more in-depth discussions of the topics covered here, see the following resources.

Bodies immersed in viscous flows.

- Happel & Brenner, Low Reynolds Number Hydrodynamics.
- Kim & Karrila, Microhydrodynamics.

Basics of complex fluids.

- Bird, Armstrong & Hassager, Dynamics of Polymeric Liquids, Vol 1.
- Graham, Microhydrodynamics, Brownian Motion and Complex Fluids.
- Larson, The Structure and Rheology of Complex Fluids.
- Morozov & Spagnolie, Chapter 1 of Complex Fluids in Biological Systems.

Kinetic theory.

- Bird, Curtiss, Armstrong & Hassager, Dynamics of Polymeric Liquids, Vol 2.
- Doi & Edwards, The Theory of Polymer Dynamics.

2 Lecture 1: From Batchelor's formula to Einstein's effective viscosity

Our first step into the world of complex fluids takes us back to a famous result by Einstein in 1906[4]. We will compute the extra stress associated with a dilute suspension of rigid spheres in a viscous solvent. Einstein used an energy dissipation argument, but we are going to take the scenic route. Down this road are numerous building blocks and ideas that will help us generalize and extend the calculation to more complex systems, starting in Lecture 2.

As noted in the introduction, a *quasi-Newtonian* fluid is one for which the stress tensor is still a constant times the local rate-of-strain tensor. This means that the extra stress must take the simple form $\mathbf{\Sigma} = 2\mu'\mathbf{E}$, for some added constant viscosity μ'. The most famous example of a quasi-Newtonian fluid is the fluid advertised above. Einstein showed for small particle volume fraction, ϕ, ($\phi = N(4\pi a^3/3)/V$ for N spheres of radius a per volume V), that $\mu' = \mu(\frac{5}{2}\phi + O(\phi^2))$. Why should it depend on the solvent viscosity, μ? It's because the effect of a particle's presence is to counteract forces acting upon it from the solvent, so as to remain rigid. Let's make this precise.

2.1 Reduction to a surface integral: the stresslet

We will follow the path forged by Batchelor (1970). Consider a control volume V just large enough so that any averaged quantities vary smoothly in space (a 'representative volume element'). The effective stress is the (local) volume average of the true stress,

$$\boldsymbol{\sigma}_{\text{eff}} = \frac{1}{V}\int_V \boldsymbol{\sigma}\,\mathrm{d}v, \tag{2.1}$$

where $\mathrm{d}v$ is an infinitesimal volume element. If there are N bodies in V, taking up volume in regions denoted by V_n, we can write

$$\boldsymbol{\sigma}_{\text{eff}} = \frac{1}{V}\left(\int_{V\setminus\cup V_n} \boldsymbol{\sigma}\,\mathrm{d}v + \sum_{n=1}^{N}\int_{V_n}\boldsymbol{\sigma}\,\mathrm{d}v\right). \tag{2.2}$$

We will tackle these integrals separately. But let us first also define the locally averaged rate-of-strain in the representative volume element,

$$\langle\mathbf{E}\rangle := \frac{1}{V}\int_V \mathbf{E}\,\mathrm{d}v = \frac{1}{V}\left(\int_{V\setminus\cup V_n}\mathbf{E}\,\mathrm{d}v + \sum_{n=1}^{N}\int_{V_n}\mathbf{E}\,\mathrm{d}v\right). \tag{2.3}$$

The first integral. The first integral in (2.2) is taken over the solvent volume, so the integrand is just the Newtonian (solvent) stress, $\boldsymbol{\sigma} = \boldsymbol{\sigma}_S := -p\mathbf{I} + 2\mu\mathbf{E}$, and we have

$$\begin{aligned}\int_{V\setminus\cup V_n}\boldsymbol{\sigma}_S\,\mathrm{d}v &= \left(-\int_{V\setminus\cup V_n} p\,\mathrm{d}v\right)\mathbf{I} + 2\mu\int_{V\setminus\cup V_n}\mathbf{E}\,\mathrm{d}v\\ &= \left(-\int_{V\setminus\cup V_n} p\,\mathrm{d}v\right)\mathbf{I} + 2\mu\left(V\langle\mathbf{E}\rangle - \sum_{n=1}^{N}\int_{V_n}\mathbf{E}\,\mathrm{d}v\right).\end{aligned} \tag{2.4}$$

We could insert a rigid body motion for the velocity field *internal* to each body, but it is more convenient to use the divergence theorem, so that everything can be computed using only the external velocity field. Using the divergence theorem, we have

$$2\mu\int_{V_n} E_{ij}\,\mathrm{d}v = \mu\int_{V_n}\partial_i u_j + \partial_j u_i\,\mathrm{d}v = \mu\int_{S_n}\nu_i u_j + \nu_j u_i\,\mathrm{d}S, \tag{2.5}$$

[4] A follow-up work in 1911 by the same author corrected an error in the first paper. Nobody's perfect.

where $\boldsymbol{\nu}$ is the normal vector on a particle surface pointing into the fluid, S_n denotes the surface of particle n, and dS is an infinitesimal surface area element. Or, in vector notation,

$$2\mu \int_{V_n} \mathbf{E}\,\mathrm{d}v = \mu \int_{S_n} (\boldsymbol{\nu}\boldsymbol{u} + \boldsymbol{u}\boldsymbol{\nu})\,\mathrm{d}S. \tag{2.6}$$

The second integral. Moving on to the second integral in (2.2), we would seem to need the stress tensor inside of each immersed body. Momentum balance inside a body would be given by $\rho_s \mathrm{D}\boldsymbol{u}/\mathrm{D}t = \nabla \cdot \boldsymbol{\sigma} + \rho_s \boldsymbol{b}$, where $\rho_s \boldsymbol{b}$ is a body force per volume, and ρ_s is the (solid) body density. If particle n is undergoing rigid body motion, then internal to the body the velocity field is $\boldsymbol{u}(\boldsymbol{x}, t) = \boldsymbol{U} + \boldsymbol{\Omega}(t) \times (\boldsymbol{x} - \boldsymbol{X})$, where $\boldsymbol{X}(t)$ is its centroid, $\boldsymbol{X}(t) = |V_n|^{-1} \int_{V_n(t)} \boldsymbol{x}\,\mathrm{d}v$. For rigid body motion, then, we have in a frame moving with the material the acceleration

$$\frac{\mathrm{D}\boldsymbol{u}}{\mathrm{D}t} = \dot{\boldsymbol{U}} + \dot{\boldsymbol{\Omega}} \times (\boldsymbol{x} - \boldsymbol{X}) + \boldsymbol{\Omega} \times (\boldsymbol{\Omega} \times (\boldsymbol{x} - \boldsymbol{X})), \tag{2.7}$$

or, defining the operator $\hat{\Omega} = \boldsymbol{\Omega}\times$,

$$\frac{\mathrm{D}\boldsymbol{u}}{\mathrm{D}t} = \dot{\boldsymbol{U}} + (\dot{\hat{\Omega}} + \hat{\Omega}^2) \cdot (\boldsymbol{x} - \boldsymbol{X}). \tag{2.8}$$

Do we really need to calculate $\boldsymbol{\sigma}$ inside each body? For rigid body motion, we don't! We can instead move the second integral in (2.2) to the boundary, where Newton's third law allows us to replace the internal stresses with external tractions, which depend only on the solvent dynamics. The divergence theorem gives:

$$\begin{aligned} \int_{V_n} \sigma_{ij}\,\mathrm{d}v &= \int_{V_n} \partial_k[(x_i - X_i)\sigma_{kj}] - (x_i - X_i)\partial_k \sigma_{kj}\,\mathrm{d}v \\ &= \int_{S_n} (x_i - X_i)\nu_k \sigma_{kj}\,\mathrm{d}S - \int_{V_n} (x_i - X_i)\left\{\rho_s(\boldsymbol{x})\left(\frac{\mathrm{D}\boldsymbol{u}}{\mathrm{D}t}\right)_j - \rho_s(\boldsymbol{x}) b_j\right\}\mathrm{d}v. \end{aligned} \tag{2.9}$$

Writing the traction from the fluid outside the particle as $\boldsymbol{f} = \boldsymbol{\nu} \cdot \boldsymbol{\sigma}_S$, by Newton's third law we have on the surface S_n that $\boldsymbol{\nu} \cdot \boldsymbol{\sigma}_S + (-\boldsymbol{\nu}) \cdot \boldsymbol{\sigma} = \mathbf{0}$, or $\nu_k \sigma_{kj} = f_j$. Inserting the rigid body acceleration from (2.8), we then arrive at

$$\int_{V_n} \boldsymbol{\sigma}\,\mathrm{d}v = \int_{S_n} (\boldsymbol{x} - \boldsymbol{X})\boldsymbol{f}\,\mathrm{d}S - \int_{V_n} \rho_s(\boldsymbol{x})(\boldsymbol{x} - \boldsymbol{X})\left\{-\boldsymbol{b} + \dot{\boldsymbol{U}} + (\dot{\hat{\Omega}} + \hat{\Omega}^2) \cdot (\boldsymbol{x} - \boldsymbol{X})\right\}\mathrm{d}v. \tag{2.10}$$

Defining the first mass moment $\boldsymbol{R}_0 := \int_{V_n} \rho_s(\boldsymbol{x})(\boldsymbol{x} - \boldsymbol{X})\,\mathrm{d}v$ (which might not be zero, since $\boldsymbol{X}$ is the centroid, not necessarily the center of mass) and the second moment of mass tensor $\mathbf{J} = \int_{V_n} \rho_s(\boldsymbol{x})(\boldsymbol{x} - \boldsymbol{X})(\boldsymbol{x} - \boldsymbol{X})\,\mathrm{d}v$, we thus have (using $\hat{\Omega} = -\hat{\Omega}^T$) that

$$\int_{V_n} \boldsymbol{\sigma}\,\mathrm{d}v = \int_{S_n} (\boldsymbol{x} - \boldsymbol{X})\boldsymbol{f}\,\mathrm{d}S + \left\{\boldsymbol{R}_0\left(\boldsymbol{b} - \dot{\boldsymbol{U}}\right) + \mathbf{J} \cdot (\dot{\hat{\Omega}} - \hat{\Omega}^2)\right\}. \tag{2.11}$$

Summary. Combining everything above, the effective stress is given by[5]

$$\boldsymbol{\sigma}_{\mathrm{eff}} = -p^{\mathrm{eff}}\mathbf{I} + 2\mu\langle\mathbf{E}\rangle + \boldsymbol{\Sigma}, \tag{2.12}$$

where

$$p^{\mathrm{eff}} = \frac{1}{V}\int_{V \setminus \cup V_n} p\,\mathrm{d}v - \sum_{n=1}^{N} \frac{1}{3}\mathrm{tr}(\boldsymbol{\Sigma}_n), \qquad \langle\mathbf{E}\rangle = \frac{1}{V}\int_V \mathbf{E}\,\mathrm{d}v, \qquad \boldsymbol{\Sigma} = \sum_{n=1}^{N}\left(\boldsymbol{\Sigma}_n - \frac{1}{3}\mathrm{tr}(\boldsymbol{\Sigma}_n)\mathbf{I}\right), \tag{2.13}$$

$$\boldsymbol{\Sigma}_n := \frac{1}{V}\int_{S_n} (\boldsymbol{x} - \boldsymbol{X}^n)\boldsymbol{f} - \mu(\boldsymbol{\nu}\boldsymbol{u} + \boldsymbol{u}\boldsymbol{\nu})\,\mathrm{d}S + \frac{1}{V}\left\{\boldsymbol{R}_0\left(\boldsymbol{b} - \dot{\boldsymbol{U}}^n\right) + \mathbf{J} \cdot (\dot{\hat{\Omega}} - \hat{\Omega}^2)\right\}_n, \tag{2.14}$$

[5] When you see a constitutive law for a complex fluid in the wild, it is likely that the final, effective stress is simply written as $\boldsymbol{\sigma}$, the effective pressure as p, and the effective rate-of-strain tensor, $\langle\mathbf{E}\rangle$, as $\mathbf{E}$!

where $\boldsymbol{X}^n$ is the centroid of the nth particle. We have subtracted off the trace of the extra stress and lumped it into the pressure. p^{eff} is again to be considered a Lagrange multiplier which enforces incompressibility, $\nabla \cdot \boldsymbol{u} = 0$.

Keeping the inertial terms on the right will take us into Maxey-Riley territory (Maxey and Riley, 1983), where particle inertia may still be present even if the surrounding solvent remains well modeled as zero Reynolds number (Stokes) flow. In that case, expressions for the translational/rotational velocities, and accelerations are needed, resulting in memory kernels and other challenges. We are going to assume that these inertial effects are negligibly small, but they were included up to this point for the sake of completeness. I hope you enjoyed the ride.

For rigid body motion, if the no-slip boundary condition holds on the particle surface, the surface velocity term in $\boldsymbol{\Sigma}_n$ is zero. To see this, writing $\boldsymbol{u} = \boldsymbol{U} + \hat{\Omega} \cdot (\boldsymbol{x} - \boldsymbol{X})$ on the surface of particle n, we can use

$$\int_{S_n} \boldsymbol{\nu} \, \mathrm{d}S = \int_{S_n} \boldsymbol{\nu} \cdot \mathbf{I} \, \mathrm{d}S = \int_{V_n} \nabla \cdot \mathbf{I} \, \mathrm{d}v = \mathbf{0}, \tag{2.15}$$

and

$$\begin{aligned} \int_{S_n} \hat{\Omega}_{ik}(x_k - X_k)\nu_j + \nu_i \hat{\Omega}_{jk}(x_k - X_k) \, \mathrm{d}S &= \int_{V_n} \hat{\Omega}_{ik}\partial_j(x_k - X_k) + \hat{\Omega}_{jk}\partial_i(x_k - X_k) \, \mathrm{d}v \\ &= \int_{V_n} \hat{\Omega}_{ij} + \hat{\Omega}_{ji} \, \mathrm{d}v = 0, \end{aligned} \tag{2.16}$$

which leads to the promised result, $\int_{S_n} \boldsymbol{\nu}\boldsymbol{u} + \boldsymbol{u}\boldsymbol{\nu} \, \mathrm{d}S = \mathbf{0}$. The contribution to the stress due to particle n is then very clean. The particle contributes only the first moment of its surface traction,

$$\boxed{\boldsymbol{\Sigma}_n = \frac{1}{V} \int_{S_n} (\boldsymbol{x} - \boldsymbol{X}^n) \, \boldsymbol{f} \, \mathrm{d}S,} \tag{2.17}$$

which is Batchelor's formula for the particle stress in a suspension (Batchelor, 1970). It is common to absorb the trace into the pressure. The traceless part of the above, which we write as $[\boldsymbol{\Sigma}_n] := \boldsymbol{\Sigma}_n - \frac{1}{3}\mathrm{tr}(\boldsymbol{\Sigma}_n)\mathbf{I}$, is the *stresslet* density: it encodes how much the rigid particle must "fight back" against the straining flow to satisfy the no-slip boundary condition. (*Must* we throw the isotropic part into the pressure? No.)

Einstein's calculation is the evaluation of (2.17) for one sphere, followed by a sum over a dilute, non-interacting population, which we tackle in the next section. But there are situations in which some of the other integrals above do not vanish. If the particles are active, for instance if they are swimming with a tangential surface velocity field (e.g. in ciliary locomotion, or diffusiophoretic motion), the surface velocity integral generally contributes a nonzero stresslet (see Blake, 1971; Ishikawa et al., 2006; Spagnolie and Lauga, 2012; Michelin and Lauga, 2014; Pak and Lauga, 2014; Saintillan, 2018 to get started); and the Maxey-Riley inertial contributions are considered for active particles by Wang and Ardekani (2012).

2.2 The disturbance flow due to a single spherical particle

Consider a background velocity field, $\boldsymbol{u}^\infty(\boldsymbol{x})$, which is assumed to vary slowly relative to the size of the particle with centroid $\boldsymbol{X}$. Expanding locally, we have

$$\boldsymbol{u}^\infty(\boldsymbol{x}) \approx \boldsymbol{u}^\infty(\boldsymbol{X}) + (\boldsymbol{x} - \boldsymbol{X}) \cdot \mathbf{A}^\infty, \tag{2.18}$$

where $\mathbf{A}^\infty = \nabla \boldsymbol{u}^\infty(\boldsymbol{X}) = \mathbf{E}^\infty + \mathbf{W}^\infty$ (see (1.6)). $\mathbf{A}^\infty$, $\mathbf{E}^\infty$ and $\mathbf{W}^\infty$ are assumed to be constant across the representative volume element, and recall that $\boldsymbol{r} \cdot \mathbf{W}^\infty = \frac{1}{2}\boldsymbol{\omega}^\infty \times \boldsymbol{r}$.

The sphere, a rigid body, translates and rotates with velocity $\boldsymbol{U}$ and rotational velocity $\boldsymbol{\Omega}$. Faxén's laws relate the viscous force $\boldsymbol{F}_v$ and torque $\boldsymbol{L}_v$ acting on the body to the undisturbed flow field,

$$\boldsymbol{F}_v = -6\pi\mu a\left(\boldsymbol{U} - \left(1 + \frac{a^2}{6}\nabla^2\right)\boldsymbol{u}^\infty(\boldsymbol{X})\right), \quad \boldsymbol{L}_v = -8\pi\mu a^3\left(\boldsymbol{\Omega} - \frac{1}{2}\boldsymbol{\omega}^\infty(\boldsymbol{X})\right), \tag{2.19}$$

where $\boldsymbol{\omega}^\infty = \nabla \times \boldsymbol{u}^\infty$ is the vorticity of the background flow (see Kim and Karrila (1991)). Any external force and torque acting on the sphere, $\boldsymbol{F}$ and $\boldsymbol{L}$, balance these viscous effects (assuming the zero Reynolds number limit and no Maxey-Riley-type inertial contributions), or $\boldsymbol{F} + \boldsymbol{F}_v = \boldsymbol{0}$ and $\boldsymbol{L} + \boldsymbol{L}_v = \boldsymbol{0}$.

Assuming zero external forces and torques, the rigid sphere thus translates with the background flow, $\boldsymbol{U} = \boldsymbol{u}^\infty(\boldsymbol{X}) + O(a^2\nabla^2\boldsymbol{u}^\infty)$, and has a rotational velocity equal to half the local vorticity, $\boldsymbol{\Omega} = \frac{1}{2}\boldsymbol{\omega}^\infty$. A sphere which rotates at this rate would perfectly match the fluid velocity of the imposed velocity field on its boundary, and so be invisible to the flow, if the background flow had no symmetric part (i.e. if $\mathbf{E}^\infty = \boldsymbol{0}$). So, by the linearity of the Stokes equations and the principle of linear superposition, the only contribution to the stresslet must be from the straining ($\mathbf{E}^\infty$) part of the flow. The straining part of the flow would stretch/squeeze a spherical volume element along its (orthogonal) principal axes. The rigid sphere resists this stretching, which does affect the fluid flow.

We will write the velocity field as $\boldsymbol{u}(\boldsymbol{x}) = \boldsymbol{u}^\infty(\boldsymbol{x}) + \boldsymbol{u}^d(\boldsymbol{x})$, where $\boldsymbol{u}^d$ is the disturbance flow due to the presence of the sphere. Naturally, $\boldsymbol{u}^d$ must also solve the Stokes equations (along with some pressure p^d), and the no-slip boundary condition requires that $\boldsymbol{U} + \boldsymbol{\Omega} \times (\boldsymbol{x} - \boldsymbol{X}) = \boldsymbol{u}^\infty(\boldsymbol{x}) + \boldsymbol{u}^d(\boldsymbol{x})$ for points $\boldsymbol{x}$ on the surface of the sphere, $|\boldsymbol{x} - \boldsymbol{X}| = a$, and $\boldsymbol{u}^d \to \boldsymbol{0}$ as $|\boldsymbol{x} - \boldsymbol{X}| \to \infty$.

2.3 The singularity method for Stokes flow (Green's functions)

Problems in Stokes flow can often be solved by the singularity method, placing fundamental singularities and their derivatives inside a body (this is an old idea, but see Chwang and Wu (1975) for a brilliant application). The exact disturbance flow for a sphere in a linear background flow is given in this way by placing a Stokeslet, source dipole, rotlet, and stresslet singularities at the center of the sphere. First, we have the *Stokeslet*, the fundamental solution associated with placing a point force $\boldsymbol{F}$ in the fluid at a point $\boldsymbol{X}$. By the linearity of the incompressible Stokes equations ($-\nabla p + \mu\nabla^2\boldsymbol{u} = \boldsymbol{0}$, $\nabla \cdot \boldsymbol{u} = 0$), it must be that we can write

$$\boldsymbol{u}^d(\boldsymbol{x}) = \frac{1}{8\pi\mu}\boldsymbol{F} \cdot \mathbf{G}(\boldsymbol{x}; \boldsymbol{X}), \tag{2.20}$$

a linear relation between the vectors $\boldsymbol{F}$ and $\boldsymbol{u}$, encoded by a free-space Green's function, $\mathbf{G}$. $\mathbf{G}$ is the Stokeslet singularity, which is given by

$$\mathbf{G}(\boldsymbol{x}; \boldsymbol{X}) = \left(\frac{\mathbf{I}}{r} + \frac{\boldsymbol{r}\boldsymbol{r}}{r^3}\right), \tag{2.21}$$

with $\boldsymbol{r} = \boldsymbol{x} - \boldsymbol{X}$ and $r = |\boldsymbol{r}|$. The associated pressure field is $p^d(\boldsymbol{x}) = (\boldsymbol{F}/8\pi) \cdot \boldsymbol{\Pi}$, where

$$\boldsymbol{\Pi} = \frac{2\boldsymbol{r}}{r^3}. \tag{2.22}$$

Derivatives of the Stokeslet also solve the Stokes equations, and a multipole expansion takes the form

$$8\pi\mu u_j^d(\boldsymbol{x}) = F_i G_{ij}(\boldsymbol{x}; \boldsymbol{X}) + D_{ik} G_{ij,k}(\boldsymbol{x}; \boldsymbol{X}) + ..., \tag{2.23}$$

where $G_{ij,k} := \partial_k G_{ij}$, or, defining $\mathbf{D} : \nabla\mathbf{G} = D_{ik} G_{ij,k}$,

$$8\pi\mu\boldsymbol{u}^d(\boldsymbol{x}) = \boldsymbol{F} \cdot \mathbf{G}(\boldsymbol{x}; \boldsymbol{X}) + \mathbf{D} : \nabla\mathbf{G}(\boldsymbol{x}; \boldsymbol{X}) + ... \tag{2.24}$$

We decompose the coefficient tensor $\mathbf{D}$ into an isotropic part, a traceless symmetric part, $\mathbf{S}$, and an antisymmetric part, $\mathbf{T}$,

$$\mathbf{D} = \frac{1}{3}\mathrm{tr}(\mathbf{D})\mathbf{I} + \mathbf{S} + \mathbf{T}, \tag{2.25}$$

where $\mathrm{tr}(\mathbf{S}) = \mathrm{tr}(\mathbf{T}) = 0$. $\mathbf{S}$ is also called... the *stresslet*. So I sure hope that $\mathbf{S}$ is related to the stresslet in (2.17)! Stay tuned. The antisymmetric part results in a velocity field which can be written in terms of a single vector, $\boldsymbol{L}$, (defined such that $T_{ik} = \varepsilon_{ik\ell}L_\ell$) and the rotlet tensor, $\mathbf{G}^c(\boldsymbol{x};\boldsymbol{X})$, where

$$T_{ik}G_{ij,k}(\boldsymbol{x};\boldsymbol{X}) = \varepsilon_{ik\ell}L_\ell G_{ij,k}(\boldsymbol{x};\boldsymbol{X}) = -L_\ell\varepsilon_{\ell ki}G_{ij,k}(\boldsymbol{x};\boldsymbol{X}), \tag{2.26}$$

$$\Rightarrow 8\pi\mu\boldsymbol{u}^d = \boldsymbol{L}\cdot\mathbf{G}^c(\boldsymbol{x};\boldsymbol{X}) := -\boldsymbol{L}\cdot(\nabla\times\mathbf{G}) = \frac{\boldsymbol{L}\times\boldsymbol{r}}{r^3}. \tag{2.27}$$

This vector $\boldsymbol{L}$ represents the torque acting on the fluid (or minus the viscous torque of the fluid acting upon the body).

An incredibly useful fact is that the fluid velocity due to the presence of a sphere in a linear background flow can be written in terms of just a handful of singularities:

$$8\pi\mu\boldsymbol{u}^d(\boldsymbol{x}) = \boldsymbol{F}\cdot\left(1+\frac{a^2}{6}\nabla^2\right)\mathbf{G}(\boldsymbol{x};\boldsymbol{X}) + \boldsymbol{L}\cdot\mathbf{G}^c(\boldsymbol{x};\boldsymbol{X}) + \mathbf{S}:\left(1+\frac{a^2}{10}\nabla^2\right)\nabla\mathbf{G}(\boldsymbol{x};\boldsymbol{X}), \tag{2.28}$$

or

$$8\pi\mu u_j^d = F_i\left(1+\frac{a^2}{6}\nabla^2\right)G_{ij} + L_iG^c_{ij} + S_{ik}\left(1+\frac{a^2}{10}\nabla^2\right)G_{ij,k}. \tag{2.29}$$

This is not just the first few terms in an expansion, this will be exact when we select $\boldsymbol{F}$, $\boldsymbol{L}$, and $\mathbf{S}$ appropriately. Here, $\nabla^2\mathbf{G}$ are source dipoles (potential doublets), and $\nabla^2(\nabla\mathbf{G})$ are a particular set of source quadrupoles (or equivalently, force octupoles). Note that (setting $\boldsymbol{X} = \mathbf{0}$ for the sake of clarity),

$$\boldsymbol{F}\cdot\left(1+\frac{a^2}{6}\nabla^2\right)\mathbf{G}\Big|_{r=a} = \frac{4}{3a}\boldsymbol{F}, \tag{2.30}$$

$$\boldsymbol{L}\cdot\mathbf{G}^c = \frac{\boldsymbol{L}\times\boldsymbol{r}}{r^3}, \tag{2.31}$$

$$G_{ij,k} = \frac{1}{r^3}\left(-\delta_{ij}r_k + \delta_{ik}r_j + \delta_{jk}r_i\right) - \frac{3r_ir_jr_k}{r^5}, \tag{2.32}$$

$$\nabla^2G_{ij,k} = \frac{-6}{r^5}\left(\delta_{ij}r_k + \delta_{jk}r_i + \delta_{ik}r_j\right) + \frac{30r_ir_jr_k}{r^7}, \tag{2.33}$$

$$\left(1+\frac{a^2}{10}\nabla^2\right)G_{ij,k}\Big|_{r=a} = \frac{2}{5a^3}\left(-4\delta_{ij}r_k + \delta_{jk}r_i + \delta_{ik}r_j\right). \tag{2.34}$$

See Kim and Karrila (1991). If there are no external forces or torques acting on the sphere, then $\boldsymbol{F} = \boldsymbol{L} = \mathbf{0}$, and in that case the body translates with the background flow and rotates with half the vorticity according to (2.19). Using that $\mathrm{tr}(\mathbf{S}) = 0$ and $\mathbf{S}^T = \mathbf{S}$, we have that

$$8\pi\mu u_j^d\Big|_{r=a} = S_{ik}\left(1+\frac{a^2}{10}\nabla^2\right)G_{ij,k}\Big|_{r=a} = \frac{2}{5a^3}\left(-4r_kS_{jk} + r_iS_{ij} + S_{ii}r_j\right) = \frac{-6}{5a^3}r_iS_{ij}. \tag{2.35}$$

Finally, to satisfy the no-slip boundary condition, we still require $\boldsymbol{u}^d = -\boldsymbol{r}\cdot\mathbf{E}^\infty$ on the surface of the rotating sphere, which is obtained when

$$\mathbf{S} = \frac{20\pi\mu a^3}{3}\mathbf{E}^\infty. \tag{2.36}$$

The total disturbance flow due to the presence of the force- and torque-free (translating and rotating) sphere is thus given by

$$8\pi\mu \boldsymbol{u}^d(\boldsymbol{x}) = \mathbf{S} : \left(1 + \frac{a^2}{10}\nabla^2\right) \nabla \mathbf{G}(\boldsymbol{x}; \boldsymbol{X}), \tag{2.37}$$

with $\mathbf{S}$ given above.

2.4 Computing the surface traction, and the extra particle stress

We can now compute the extra particle stress, from (2.17). We need the surface traction, $\boldsymbol{f} = \boldsymbol{\nu} \cdot \boldsymbol{\sigma}_S = \boldsymbol{\nu} \cdot (-p\mathbf{I} + 2\mu\mathbf{E})$, where $\boldsymbol{\nu} = \boldsymbol{r}/a$, $p = p^\infty + p^d(\boldsymbol{x})$, and $\mathbf{E} = \mathbf{E}^\infty + \mathbf{E}^d(\boldsymbol{x})$. The pressure field associated with the Stokeslet is harmonic, so many terms vanish (e.g. the source doublet and rotlet are zero pressure flows). Ultimately, accompanying (2.28), we have (using that $\mathbf{S} = \mathbf{S}^T$) simply that

$$8\pi p^d(\boldsymbol{x}) = \boldsymbol{F} \cdot \boldsymbol{\Pi} + \mathbf{S} : \nabla \boldsymbol{\Pi}, \tag{2.38}$$

where $\boldsymbol{F} = \mathbf{0}$ in our force free consideration, and

$$\nabla \boldsymbol{\Pi} = \frac{2}{r^3}\left(\mathbf{I} - \frac{3\boldsymbol{r}\boldsymbol{r}}{r^2}\right). \tag{2.39}$$

So, on the surface of the sphere, since $\mathbf{S} : \mathbf{I} = \mathrm{tr}(\mathbf{S}) = 0$, we have

$$p^d(\boldsymbol{x}) = \frac{-3}{4\pi a^5}\mathbf{S} : \boldsymbol{r}\boldsymbol{r}. \tag{2.40}$$

The elements of the rate-of-strain tensor are given by

$$E_{jm} = E^\infty_{jm} + \frac{1}{8\pi\mu} S_{ik}\left(1 + \frac{a^2}{10}\nabla^2\right)\left(\frac{\partial_m G_{ij,k} + \partial_j G_{im,k}}{2}\right)\Big|_{r=a}. \tag{2.41}$$

To compute this we will need

$$\begin{aligned}\partial_m G_{ij,k} = {} & \frac{1}{r^3}\left(-\delta_{ij}\delta_{km} + \delta_{ik}\delta_{jm} + \delta_{jk}\delta_{im}\right) \\ & - \frac{3\left(-\delta_{ij}r_k r_m + \delta_{ik}r_j r_m + \delta_{jk}r_i r_m + \delta_{im}r_j r_k + \delta_{jm}r_i r_k + \delta_{km}r_i r_j\right)}{r^5} + \frac{15 r_i r_j r_k r_m}{r^7}.\end{aligned} \tag{2.42}$$

Using $\mathrm{tr}(\mathbf{S}) = 0$ and $\mathbf{S} = \mathbf{S}^T$, we have

$$S_{ik}\partial_m G_{ij,k} = \frac{-3\left(2r_j S_{mk} r_k + (\mathbf{S} : \boldsymbol{r}\boldsymbol{r})\delta_{jm}\right)}{r^5} + \frac{15 S_{ik} r_i r_j r_k r_m}{r^7}, \tag{2.43}$$

so, with $[\cdot]^{sym}$ denoting the symmetric part, we have

$$\mathbf{C} := \left[\nabla\left(\mathbf{S} : \nabla \mathbf{G}\right)\right]^{sym} = \frac{-3\boldsymbol{r}(\mathbf{S}\cdot\boldsymbol{r}) - 3(\mathbf{S}\cdot\boldsymbol{r})\boldsymbol{r} - 3(\mathbf{S} : \boldsymbol{r}\boldsymbol{r})\mathbf{I}}{r^5} + \frac{15(\mathbf{S} : \boldsymbol{r}\boldsymbol{r})\boldsymbol{r}\boldsymbol{r}}{r^7}. \tag{2.44}$$

Since the Laplacian commutes with the del operator, we can just compute from here that

$$\nabla^2 \mathbf{C} = -\frac{12}{r^5}\mathbf{S} + \frac{60\left((\mathbf{S}\cdot\boldsymbol{r})\boldsymbol{r} + \boldsymbol{r}(\mathbf{S}\cdot\boldsymbol{r})\right) + 30(\mathbf{S} : \boldsymbol{r}\boldsymbol{r})\mathbf{I}}{r^7} - \frac{210(\mathbf{S} : \boldsymbol{r}\boldsymbol{r})\boldsymbol{r}\boldsymbol{r}}{r^9}. \tag{2.45}$$

Thus, we have on the sphere surface that

$$\mathbf{E}^d(\boldsymbol{x}) = \frac{1}{8\pi\mu}\left(\mathbf{C} + \frac{a^2}{10}\nabla^2\mathbf{C}\right)_{r=a} \tag{2.46}$$

$$= \frac{1}{8\pi\mu a^3}\left(-\frac{6}{5}\mathbf{S} + 3\left[\boldsymbol{\nu}(\mathbf{S}\cdot\boldsymbol{\nu}) + (\mathbf{S}\cdot\boldsymbol{\nu})\boldsymbol{\nu}\right] - 6(\mathbf{S} : \boldsymbol{\nu}\boldsymbol{\nu})\boldsymbol{\nu}\boldsymbol{\nu}\right). \tag{2.47}$$

Inserting the disturbance pressure from (2.40), we find the traction

$$\boldsymbol{f} = \boldsymbol{\nu} \cdot (-p\mathbf{I} + 2\mu\mathbf{E}) = -p^\infty \boldsymbol{\nu} + \frac{3}{4\pi a^3}(\mathbf{S} : \boldsymbol{\nu}\boldsymbol{\nu})\boldsymbol{\nu} + 2\mu\boldsymbol{\nu} \cdot \left(\mathbf{E}^\infty + \mathbf{E}^d(\boldsymbol{x})\right). \tag{2.48}$$

Finally, we can compute the integral in (2.17) over the unit sphere. Using

$$\int_{\partial B(0,1)} \boldsymbol{\nu}\boldsymbol{\nu}\,\mathrm{d}S = \int_{B(0,1)} \mathbf{I}\,\mathrm{d}v = (4\pi/3)\mathbf{I}, \tag{2.49}$$

$$\int_{\partial B(0,1)} (\mathbf{S} \cdot \boldsymbol{\nu})\boldsymbol{\nu}\,\mathrm{d}S = \int_{B(0,1)} \mathbf{S}\,\mathrm{d}v = \frac{4\pi}{3}\mathbf{S}, \tag{2.50}$$

$$\int_{\partial B(0,1)} (\mathbf{S} : \boldsymbol{\nu}\boldsymbol{\nu})\mathbf{I}\,\mathrm{d}S = \frac{4\pi}{3}\mathrm{tr}(\mathbf{S})\mathbf{I} = \mathbf{0}, \tag{2.51}$$

and (with $\mathrm{tr}(\mathbf{S}) = 0$)

$$\int_{\partial B(0,1)} (\mathbf{S} : \boldsymbol{\nu}\boldsymbol{\nu})\boldsymbol{\nu}\boldsymbol{\nu}\,\mathrm{d}S = \int_{B(0,1)} (\mathbf{S} : \boldsymbol{\nu}\boldsymbol{\nu})\mathbf{I} + (\mathbf{S} \cdot \boldsymbol{\nu})\boldsymbol{\nu} + \boldsymbol{\nu}(\mathbf{S} \cdot \boldsymbol{\nu})\,dv = \frac{8\pi}{15}\mathbf{S}, \tag{2.52}$$

since $V\boldsymbol{\Sigma}_n = \int_{S_n} (\boldsymbol{x} - \boldsymbol{X})\boldsymbol{f}\,\mathrm{d}S_a = a^3 \int_{\partial B(0,1)} \boldsymbol{\nu}\boldsymbol{f}\,\mathrm{d}S$, we find that

$$\begin{aligned} V\boldsymbol{\Sigma}_n = &-\frac{4\pi a^3}{3}p^\infty\mathbf{I} + \int_{\partial B(0,1)} \frac{3}{4\pi}(\mathbf{S} : \boldsymbol{\nu}\boldsymbol{\nu})\boldsymbol{\nu}\boldsymbol{\nu} + 2\mu a^3(\mathbf{E}^\infty \cdot \boldsymbol{\nu})\boldsymbol{\nu}\,\mathrm{d}S \\ &+ \frac{1}{4\pi}\int_{\partial B(0,1)} -\frac{6}{5}(\mathbf{S} \cdot \boldsymbol{\nu})\boldsymbol{\nu} + 3(\mathbf{S} : \boldsymbol{\nu}\boldsymbol{\nu})\boldsymbol{\nu}\boldsymbol{\nu} + 3(\mathbf{S} \cdot \boldsymbol{\nu})\boldsymbol{\nu} - 6(\mathbf{S} : \boldsymbol{\nu}\boldsymbol{\nu})\boldsymbol{\nu}\boldsymbol{\nu}\,\mathrm{d}S \\ &= -\frac{4\pi a^3}{3}p^\infty\mathbf{I} + \frac{2}{5}\mathbf{S} + \frac{8\pi\mu a^3}{3}\mathbf{E}^\infty + \frac{1}{5}\mathbf{S} = -\frac{4\pi a^3}{3}p^\infty\mathbf{I} + \frac{8\pi\mu a^3}{3}\mathbf{E}^\infty + \frac{3}{5}\mathbf{S}. \end{aligned} \tag{2.53}$$

Inserting the stresslet $\mathbf{S}$ from (2.36), we finally arrive at

$$V\boldsymbol{\Sigma}_n = -\frac{4\pi a^3}{3}p^\infty\mathbf{I} + \frac{20}{3}\pi\mu a^3\mathbf{E}^\infty. \tag{2.54}$$

The traceless part of the above simply removes the first term ($\mathbf{E}^\infty$ is trace-free if the velocity field is divergence free), so:

$$V[\boldsymbol{\Sigma}_n] = V\left(\boldsymbol{\Sigma}_n - \frac{1}{3}\mathrm{tr}(\boldsymbol{\Sigma}_n)\mathbf{I}\right) = \frac{20}{3}\pi\mu a^3\mathbf{E}^\infty = \mathbf{S}. \tag{2.55}$$

So, the "stresslet" in (2.17) is...the "stresslet" (2.25), and the world is pure and good. (The traceless part of the surface moment in (2.17) is exactly the singularity stresslet $\mathbf{S}$, which has units of force times length, with $[\boldsymbol{\Sigma}_n] = \mathbf{S}/V$ its contribution per unit volume, with units of force per area, or stress). Finally, we sum the independent effects of N non-interactive particles in the control volume V. The p^∞ contributions are absorbed into the pressure, p, and we find (with $\phi = \frac{4}{3}\pi a^3 N/V$),

$$\boldsymbol{\Sigma} = 5\phi\mu\mathbf{E}^\infty, \tag{2.56}$$

resulting in a quasi-Newtonian flow with $\mu' = (5\phi/2)\mu$, and a total effective viscosity of $\left(1 + \frac{5}{2}\phi\right)\mu$. Success!

The first departure from the dilute setting results in a second-order correction, $\mu' = (\frac{5}{2}\phi + c\,\phi^2)\mu$. This calculation requires tracking the statistical locations of the spheres, and each sphere must 'see' the disturbance flows of the others. This was done in a landmark paper by Batchelor and Green (1972), who estimated the two-sphere interactions from the limiting cases of distant

spheres (far-field multipoles) and nearly-touching spheres (lubrication theory), obtaining $c = 7.6$ for a pure straining flow ($\mathbf{W}^\infty = \mathbf{0}$). Later, Yoon and Kim (1987) computed the two-sphere mobility functions at all intermediate separations, obtaining a more accurate value of $c = 6.95$. For a standard *shear* flow, which includes vorticity, the particle interactions can become closed orbits, which complicates the pairwise interaction statistics. Brownian motion destroys these closed orbits, and regularizes this calculation (see Batchelor (1977)). For a comprehensive discussion of suspension mechanics, see Guazzelli and Morris (2012).

Exercise 2.1. Given the Einstein viscosity correction, the effective viscosity is 10% larger than the solvent viscosity when $\phi = 2/50 = 4\%$. But when should we include pairwise interactions? Using the two-term expansion $\mu_{\text{eff}} = \mu(1 + \frac{5}{2}\phi + 6.95\,\phi^2)$ for a straining flow, determine the volume fraction at which the added viscosity from pairwise interactions is at least 10% as large as Einstein's added viscosity, and use that to give a range of ϕ over which the dilute (non-interacting) theory is expected to be accurate.

Exercise 2.2. Let $\boldsymbol{x} = (x, y, 0) = x\hat{\boldsymbol{x}} + y\hat{\boldsymbol{y}}$. Use $\nabla = \hat{\boldsymbol{x}}\partial_x + \hat{\boldsymbol{y}}\partial_y + \hat{\boldsymbol{z}}\partial_z$ to compute $\nabla\cdot\boldsymbol{x}$, $\nabla\boldsymbol{x}$, and $\nabla\times\boldsymbol{x}$. Next, in two dimensions using polar coordinates, writing $\boldsymbol{x} = r\hat{\boldsymbol{r}}$, use $\nabla = \hat{\boldsymbol{r}}\partial_r + \frac{1}{r}\hat{\boldsymbol{\theta}}\partial_\theta$ to compute $\nabla\cdot\boldsymbol{x}$, $\nabla\boldsymbol{x}$, and $\nabla\times\boldsymbol{x}$. (Don't forget that $\partial_\theta\hat{\boldsymbol{r}} = \hat{\boldsymbol{\theta}}$ and $\partial_\theta\hat{\boldsymbol{\theta}} = -\hat{\boldsymbol{r}}$!) Verify that you have the same results using either Cartesian or polar coordinates.

Exercise 2.3. Consider a rigid sphere of radius a, with centroid position $\boldsymbol{X}$, which translates and rotates so as to remain force and torque free. For each background flow below, find $\mathbf{A}^\infty$, $\mathbf{E}^\infty$ and $\mathbf{W}^\infty$, and $\boldsymbol{\omega}^\infty$ (see (2.18)), find the force- and torque-free translational and rotational velocities, $\boldsymbol{U}$ and $\boldsymbol{\Omega}$ in (2.19), and verify that the stresslet $\mathbf{S}$ in (2.36) is what is needed to satisfy the no-slip boundary condition (using (2.35)).

1. Solid-body rotation about $\hat{\boldsymbol{z}}$, $\boldsymbol{u}^\infty = \Omega^\infty\,(-y,\, x,\, 0)$.
2. Uniaxial straining (extensional) flow, $\boldsymbol{u}^\infty = \dot{\varepsilon}\,(-\frac{1}{2}x, -\frac{1}{2}y, z)$.
3. Planar shear flow, $\boldsymbol{u}^\infty = \dot{\gamma}\,y\,\hat{\boldsymbol{x}}$.

Exercise 2.4. Honestly, if you just work through and verify each equation in this lecture sometime, you will learn a ton.

For solutions to all exercises: *speak, friend, and enter.*

3 Lecture 2: Kinetic theory and suspensions of rods

In this lecture, we will model a suspension of slender rods in the dilute regime. If the rods are rigid, and the velocity field satisfies the no-slip boundary condition, then the extra stress is again found using Batchelor's formula, (2.17). The disturbance velocity field now depends on the rod orientation, which we denote by a unit vector $\boldsymbol{p}$. And to compute averages over the suspension we will need some statistical information about the distribution of orientations, $\psi(\boldsymbol{p}, t)$. And this in turn requires information about the dynamics of each rod's orientation. Let's get to it!

3.1 Particle distribution function and the continuity equation

A new, central object for us is the particle distribution function, which reveals the complete configuration of the particles. This is the kinetic theory approach to life: rather than track every particle individually, we follow the evolution of a distribution function over the single-particle state space, and recover macroscopic quantities as averages, or moments, of that density. Later we will see a different, empirical, approach, which takes the macroscopic quantities to be the primary building blocks, and equations of motion are guided by symmetry arguments.

In the kinetic theory approach, we will encode the 'state' of each particle in a vector, $\boldsymbol{Z}$, and the particle distribution at time t is denoted by $\psi(\boldsymbol{Z}, t)$. If the initial configurations of all the rods are known, we can treat ψ as a deterministic number density, normalized so that

$$N = \int \psi(\boldsymbol{Z}, t)\, \mathrm{d}\boldsymbol{Z}, \tag{3.1}$$

where N is the number of rods, and the integral is over the entire state space. For example, if rod-like particles are identified solely by their centroid, $\boldsymbol{X}$, and orientation, $\boldsymbol{p}$, then in three spatial dimensions we write the state as a 6-vector, $\boldsymbol{Z} = (\boldsymbol{X}, \boldsymbol{p})$, and

$$N = \int_V \int_{S^2} \psi \, \mathrm{d}\Omega \, \mathrm{d}v, \tag{3.2}$$

where V is the control volume, and $d\Omega$ is an infinitesimal solid angle (the integral is over S^2, the unit sphere, since $|\boldsymbol{p}| = 1$). (Alternatively, we could take ψ to be a probability density, normalized so that it integrates to 1, but we'll stick with N.)

If the number of particles is fixed, $dN/dt = 0$, the integral above represents a conservation law. Using the Reynolds transport theorem, we arrive at a continuity equation for ψ:

$$\partial_t \psi + \nabla_{\boldsymbol{Z}} \cdot (\dot{\boldsymbol{Z}} \psi) = 0. \tag{3.3}$$

The equation is closed by incorporating the individual particle dynamics, $\dot{\boldsymbol{Z}}$. For rods, we require $\dot{\boldsymbol{X}}$ and $\dot{\boldsymbol{p}}$, which in a dilute theory depend only on the background flow. At higher particle densities, where particle interactions cannot be neglected, then $\dot{\boldsymbol{X}}$ and $\dot{\boldsymbol{p}}$ also depend on the distribution of particles, ψ, resulting in a rich, nonlinear PDE for the distribution dynamics.

So, what are $\dot{\boldsymbol{X}}$ and $\dot{\boldsymbol{p}}$ for a dilute suspension of rigid rods? As a simplification, let us assume that the particles are very well mixed into the solvent, so that they are uniformly distributed *in space*. The associated simplification is that $\boldsymbol{Z} = \boldsymbol{p}$ and $\psi = \psi(\boldsymbol{p}, t)$, the normalization is

$$N = \int_{S^2} \psi \, \mathrm{d}\Omega, \tag{3.4}$$

and we need only investigate the orientational aspect of the dynamics, via

$$\partial_t \psi + \nabla_{\boldsymbol{p}} \cdot (\dot{\boldsymbol{p}} \psi) = 0. \tag{3.5}$$

With $\boldsymbol{p} \in S^2$, we have that $\nabla_{\boldsymbol{p}} = (\mathbf{I} - \boldsymbol{pp}) \cdot \dfrac{\partial}{\partial \boldsymbol{p}}$. We also define a per-particle average quantity as

$$\langle \boldsymbol{q} \rangle := \frac{1}{N} \int_{S^2} \boldsymbol{q} \, \psi \, \mathrm{d}\Omega. \tag{3.6}$$

Most continuum theories for macroscopic variables do not use ψ directly, but on its moments instead. For instance, the mean orientation of the N particles is computed as $\boldsymbol{n} := \langle \boldsymbol{p} \rangle$, and the second orientational moment as $\mathbf{M} := \langle \boldsymbol{pp} \rangle$. If the suspension is not far from isotropic (i.e. if ψ is nearly constant), we might try an expansion around the isotropic state in these moments, just as we might represent a probability distribution via a moment expansion:

$$\psi(\boldsymbol{p}, t) \approx \frac{N}{4\pi} \left(1 + 3\boldsymbol{n} \cdot \boldsymbol{p} + \frac{15}{2} \mathbf{M} : [\boldsymbol{pp}] + \cdots \right), \tag{3.7}$$

where $[\boldsymbol{pp}] = \boldsymbol{pp} - \frac{1}{3}\mathbf{I}$ is the traceless part of $\boldsymbol{pp}$ (as in Lecture 1). It is $[\boldsymbol{pp}]$ which appears here, not $\boldsymbol{pp}$, so that the third term is orthogonal to the first; $\int_{S^2} \boldsymbol{pp} \, \mathrm{d}\Omega = (4\pi/3)\mathbf{I}$, but $\int_{S^2} [\boldsymbol{pp}] \, \mathrm{d}\Omega = \mathbf{0}$ (see Exercises 3.4-3.5). The first orientational moment, $\boldsymbol{n} = \langle \boldsymbol{p} \rangle$ is the polar order parameter. It

features in nematic liquid crystal (LC) models, in which energies are written in terms of $\boldsymbol{n}$ and its gradients alone (e.g. an Ericksen-Leslie model LC). The traceless second moment,

$$\mathbf{Q} = [\mathbf{M}] = \langle \boldsymbol{pp} \rangle - \tfrac{1}{3}\mathbf{I}, \tag{3.8}$$

is the nematic order parameter, often called...the Q-tensor (more advanced LC theories, e.g. a Beris-Edwards model LC, active suspension models, and active nematics, are built upon $\mathbf{Q}$). See de Gennes and Prost (1993); Stewart (2019). A review of rigid and deformable bodies in nematic LCs may be found in Chandler and Spagnolie (2024).

Next, we will find the dynamics for $\dot{\boldsymbol{p}}$ in terms of the background flow using similar ideas as those used in the first lecture. But we will also include Brownian fluctuations. These are physically realistic, and also happen to be seriously important for our mathematical modeling. They regularize the distribution, and allow us to take sensible averages (otherwise the trajectories may not explore all of the configuration space, depending on their initial data).

Once we include rotational diffusivity, d (with units of inverse time), if $\dot{\boldsymbol{p}}$ is the deterministic part of the rotational dynamics, we will find

$$\partial_t \psi + \nabla_{\boldsymbol{p}} \cdot (\dot{\boldsymbol{p}}\psi) = d\nabla^2_{\boldsymbol{p}}\psi. \tag{3.9}$$

This is the Smoluchowski equation, which is the overdamped (inertialess) Fokker-Planck equation. If ψ is envisioned as a transition probability density, then this PDE is called the Forward Kolmogorov equation.

3.2 Slender body theory and orientational dynamics

Consider a rod of length L and cross-sectional radius $r(s)$, with $r(s) \in [0, a]$, and aspect ratio $\varepsilon := a/L \ll 1$, with centerline parameterized by $s \in [-L/2, L/2]$. Its centroid position and orientation are denoted by $(\boldsymbol{X}, \boldsymbol{p})$. To determine the traction, we will use slender body theory (Keller and Rubinow, 1976; Johnson, 1980), which will give an extra particle stress which is accurate up to $O(\varepsilon^2)$.

We will assume that the thickness of the rod tapers off sufficiently fast to zero at its endpoints (see the papers above, and the recent paper by Peng and Schnitzer (2026), and Mori et al. (2020); Ohm (2024) for more complete theoretical considerations). Then the mismatch between the local body velocity, $\dot{\boldsymbol{x}} = \dot{\boldsymbol{X}} + s\dot{\boldsymbol{p}}$, and the local background fluid velocity, $\boldsymbol{u}^\infty(\boldsymbol{x}(s))$, results in a local viscous force per length $\boldsymbol{F}(s)$ on the body:

$$8\pi\mu\,[\dot{\boldsymbol{x}}(s) - \boldsymbol{u}^\infty(\boldsymbol{x}(s))] = -\boldsymbol{\Lambda}(s)\cdot\boldsymbol{F}(s) - \mathbf{K}[\boldsymbol{F}](s) + O(\varepsilon^2\log(\varepsilon)\|\boldsymbol{F}\|), \tag{3.10}$$

where

$$\boldsymbol{\Lambda}(s) = c(s)(\mathbf{I} + \boldsymbol{pp}) + 2(\mathbf{I} - \boldsymbol{pp}), \tag{3.11}$$

$$\mathbf{K}[\boldsymbol{F}](s) = (\mathbf{I} + \boldsymbol{pp}) \cdot \int_{-L/2}^{L/2} \frac{\boldsymbol{F}(s) - \boldsymbol{F}(s')}{|s - s'|}\,\mathrm{d}s, \tag{3.12}$$

and

$$c(s) = \log\left(\frac{L^2 - 4s^2}{r(s)^2}\right) - 1. \tag{3.13}$$

This coefficient is why it is common in the literature to study prolate ellipsoidal particles, or $r(s) = \varepsilon\sqrt{L^2 - 4s^2}$, and then $c(s) = c = \log(1/\varepsilon^2 e)$ is a constant. We will make that choice here now as well, and then $\boldsymbol{\Lambda}$ does not vary along the rod length, and depends only on $\boldsymbol{p}$. Generally, the net viscous force and torque acting on the rod are given by

$$\boldsymbol{F}_v = \int_{-L/2}^{L/2} \boldsymbol{F}(s)\,\mathrm{d}s, \quad \boldsymbol{L}_v = \int_{-L/2}^{L/2} s\boldsymbol{p} \times \boldsymbol{F}(s)\,\mathrm{d}s. \tag{3.14}$$

In his Ph.D. thesis, Götz (2000) showed that the nonlocal integral is diagonalized by a Legendre polynomial basis. Writing $\boldsymbol{F}(s) = \sum_{k=0}^{\infty} \hat{\boldsymbol{F}}_k L_k(2s/L)$, where $L_k(z)$ is the kth Legendre polynomial on $z \in [-1, 1]$, we find that

$$\mathbf{K}[\boldsymbol{F}](s) = (\mathbf{I} + \boldsymbol{pp}) \cdot \sum_{k=1}^{\infty} \lambda_k \hat{\boldsymbol{F}}_k L_k(2s/L), \tag{3.15}$$

where $\lambda_k = 2\sum_{j=1}^{k} 1/j$ is twice the kth harmonic number.

Since the body is rigid we can write $\dot{\boldsymbol{p}} = \boldsymbol{\Omega} \times \boldsymbol{p}$, where $\boldsymbol{\Omega}$ is the rotational velocity. But we are neglecting rotation about the long axis in this theory, which corresponds to disturbance flows and tractions which are higher order in ε. So it is useful to decompose the rotational velocity into components parallel and perpendicular to $\boldsymbol{p}$: we write $\boldsymbol{\Omega} = \Omega^{||}\boldsymbol{p} + \boldsymbol{\Omega}^{\perp}$, where $\boldsymbol{p} \cdot \boldsymbol{\Omega}^{\perp} = 0$, and we won't concern ourselves with $\Omega^{||}$.

As in the previous lecture, we will consider a linear background flow (on the scale of the rod), and then $\boldsymbol{u}^{\infty}(\boldsymbol{x}(s)) \approx \boldsymbol{u}^{\infty}(\boldsymbol{X}) + s\boldsymbol{p} \cdot \mathbf{A}^{\infty}$, so

$$8\pi\mu \left[\left(\dot{\boldsymbol{X}} - \boldsymbol{u}^{\infty}(\boldsymbol{X}) \right) + s\left(\dot{\boldsymbol{p}} - \boldsymbol{p} \cdot \mathbf{A}^{\infty}\right) \right] = -\sum_{k=0}^{\infty} \left(\boldsymbol{\Lambda} + \lambda_k(\mathbf{I} + \boldsymbol{pp})\right) \cdot \hat{\boldsymbol{F}}_k L_k(2s/L), \tag{3.16}$$

where $\lambda_0 \equiv 0$. Since only constant and linear terms in s appear on the left, we therefore just have that $\boldsymbol{F}(s) = \hat{\boldsymbol{F}}_0 + (2s/L)\hat{\boldsymbol{F}}_1$. If there is no external force acting on the rod, and we neglect its inertia, then $\hat{\boldsymbol{F}}_0 = \mathbf{0}$. Integrating both sides of (3.16) then shows that $\dot{\boldsymbol{X}} = \boldsymbol{u}^{\infty}(\boldsymbol{X})$, the center of the rod moves with the background flow evaluated at that point.

Similarly, if there is no external torque acting on the rod, and we neglect its rotational inertia, then

$$\mathbf{0} = \boldsymbol{L}_v = \int_{-L/2}^{L/2} s\boldsymbol{p} \times \boldsymbol{F}(s)\,\mathrm{d}s = \int_{-L/2}^{L/2} s\boldsymbol{p} \times \left(\frac{2s}{L}\right) \hat{\boldsymbol{F}}_1\,\mathrm{d}s = \frac{L^2}{6}\boldsymbol{p} \times \hat{\boldsymbol{F}}_1. \tag{3.17}$$

Thus, $\hat{\boldsymbol{F}}_1 = \hat{F}_1^{||}\boldsymbol{p}$. Multiplying (3.16) by s and integrating yields

$$4\pi\mu L\left(\dot{\boldsymbol{p}} - \boldsymbol{p} \cdot \mathbf{A}^{\infty}\right) = -\left(\boldsymbol{\Lambda} + 2(\mathbf{I} + \boldsymbol{pp})\right) \cdot \hat{\boldsymbol{F}}_1 = -2(c+2)\hat{F}_1^{||}\boldsymbol{p}. \tag{3.18}$$

Dotting (3.18) with $\boldsymbol{p}$, and using that $\boldsymbol{p} \cdot \dot{\boldsymbol{p}} = 0$, since $|\boldsymbol{p}| = 1$, we find

$$\hat{F}_1^{||} = \frac{2\pi\mu L}{c+2}\boldsymbol{pp} : \mathbf{A}^{\infty} = \frac{2\pi\mu L}{c+2}\boldsymbol{pp} : \mathbf{E}^{\infty}, \tag{3.19}$$

the last part owing to the fact that

$$\boldsymbol{pp} : \mathbf{W}^{\infty} = p_i p_j W_{ij}^{\infty} = -p_i p_j W_{ji}^{\infty} = p_j p_i W_{ji}^{\infty} = -\boldsymbol{pp} : \mathbf{W}^{\infty}, \tag{3.20}$$

and so $\boldsymbol{pp} : \mathbf{W}^{\infty} = 0$. $\hat{F}_1^{||}$ is thus the force per length which corresponds to the resistance of the rod to being stretched by the background flow. Naturally, it is extremal when the rod is aligned with one of the principal axes of $\mathbf{E}^{\infty}$. Meanwhile, taking the cross product of (3.18) with $\boldsymbol{p}$, we find that

$$\boldsymbol{p} \times (\boldsymbol{\Omega} \times \boldsymbol{p}) = \boldsymbol{p} \times (\boldsymbol{p} \cdot \mathbf{A}^{\infty}). \tag{3.21}$$

And using $\boldsymbol{p} \times (\boldsymbol{\Omega} \times \boldsymbol{p}) = (\mathbf{I} - \boldsymbol{pp}) \cdot \boldsymbol{\Omega} = \boldsymbol{\Omega}^{\perp}$, we find that $\boldsymbol{\Omega}^{\perp} = \boldsymbol{p} \times (\boldsymbol{p} \cdot \mathbf{A}^{\infty})$, and finally that

$$\dot{\boldsymbol{p}} = \boldsymbol{\Omega}^{\perp} \times \boldsymbol{p} = (\mathbf{I} - \boldsymbol{pp}) \cdot (\boldsymbol{p} \cdot \nabla \boldsymbol{u}^{\infty}). \tag{3.22}$$

This is over a century-old result now! See Jeffery (1922). Decomposing $\mathbf{A}^\infty = \nabla \boldsymbol{u}^\infty$ into symmetric and anti-symmetric parts, this is equivalent to

$$\dot{\boldsymbol{p}} = \boldsymbol{p} \cdot \mathbf{W}^\infty + (\mathbf{I} - \boldsymbol{pp}) \cdot (\boldsymbol{p} \cdot \mathbf{E}^\infty) = \frac{1}{2}\boldsymbol{\omega}^\infty \times \boldsymbol{p} + (\mathbf{I} - \boldsymbol{pp}) \cdot (\boldsymbol{p} \cdot \mathbf{E}^\infty), \tag{3.23}$$

so the rod rotates with half the local vorticity, plus the effect of the straining flow.

As a final note, soon we will also need the rotational drag on a rod when it rotates perpendicular to $\boldsymbol{p}$ in a quiescent fluid. If the rod experiences an external torque $\boldsymbol{L}$ (so that $\boldsymbol{L} + \boldsymbol{L}_v = \mathbf{0}$), which is orthogonal to $\boldsymbol{p}$ ($\boldsymbol{L} = \boldsymbol{L}^\perp$, $\boldsymbol{L}^\perp \cdot \boldsymbol{p} = 0$) then to the above we can add (yes, just add - Stokes flow is linear, so linear superposition applies) an additional rotation rate. To find it, we can go back and set $\mathbf{A}^\infty = \mathbf{0}$ and $\dot{\boldsymbol{p}} = \boldsymbol{\Omega}^\perp \times \boldsymbol{p}$ in (3.18), and then it is easy to compute the relation $\boldsymbol{L}^\perp = -\boldsymbol{L}_v = \zeta_r \boldsymbol{\Omega}^\perp$, where

$$\zeta_r = \frac{2\pi\mu L^3}{3(c+4)}. \tag{3.24}$$

ζ_r is the rotational drag, or resistance, coefficient. So if there is an external torque acting on the rod we will add $\boldsymbol{L}^\perp/\zeta_r$ to the rotation rate in (3.22). You guessed it, this is a quick exercise. If you are concerned that there is nothing to balance a possible $\boldsymbol{p}$ directed component of $\boldsymbol{L}$, that is because we haven't been keeping $\Omega^{||}$ around. Generally, we would have $\boldsymbol{p} \cdot \boldsymbol{L} \propto \varepsilon^2 \Omega^{||}$. To be complete we could include that rotation above, but the torques we have in mind below are approximately orthogonal to $\boldsymbol{p}$, and the associated disturbance flows are often negligible. Theory which includes this rotational component was developed by Maxian and Donev (2022).

3.3 Computing the extra particle stress

We have what we need to compute the individual particle contribution to the extra stress. The traction (force per area), $\boldsymbol{f}$, needed in Batchelor's formula (2.17) is related to this force per length by $2\pi r(s)\boldsymbol{f} = \boldsymbol{F}(s)$. We can check that the total viscous force acting on the particle is zero,

$$\int_{-L/2}^{L/2} \int_0^{2\pi} \boldsymbol{f}(s,\theta) r(s) \, \mathrm{d}\theta \, \mathrm{d}s = \int_{-L/2}^{L/2} \boldsymbol{F}(s) \, \mathrm{d}s = \mathbf{0}. \tag{3.25}$$

Then, denoting the position vector on the surface relative to the centroid as $\boldsymbol{r}(s,\theta)$, we find

$$V\boldsymbol{\Sigma}_n(\boldsymbol{p},t) = \int_{-L/2}^{L/2} \int_0^{2\pi} \boldsymbol{r}(s,\theta)\boldsymbol{f}(s,\theta) r(s) \, \mathrm{d}\theta \, \mathrm{d}s = \int_{-L/2}^{L/2} s\boldsymbol{p}\boldsymbol{F}(s) \, \mathrm{d}s + O(\varepsilon) \tag{3.26}$$

$$= \frac{L^2 \hat{F}_1^{||}}{6} \boldsymbol{pp} + O(\varepsilon), \tag{3.27}$$

or

$$V\boldsymbol{\Sigma}_n(\boldsymbol{p},t) \sim \frac{2\pi\mu L^3}{6(c+2)} \boldsymbol{pppp} : \mathbf{E}^\infty \quad \text{as} \quad \varepsilon \to 0. \tag{3.28}$$

The total extra stress, $\boldsymbol{\Sigma}$, in (2.13), is a sum of the traceless part of each $\boldsymbol{\Sigma}_n$,

$$[\boldsymbol{\Sigma}_n] = \boldsymbol{\Sigma}_n - \frac{1}{3}\mathrm{tr}(\boldsymbol{\Sigma}_n)\mathbf{I} \sim \frac{2\pi\mu L^3}{6(c+2)V} \left(\boldsymbol{pppp} - \frac{1}{3}\mathbf{I}\boldsymbol{pp} \right) : \mathbf{E}^\infty, \tag{3.29}$$

over all N particles. But for the sum we need to know each particle's orientation (in the above we should really write $\boldsymbol{p}^n$ since this is the extra stress due to particle n, but wow what a mess).

Here is where we incorporate the number density, $\psi(\boldsymbol{p}, t)$, and write the weighted average extra stress as

$$\boldsymbol{\Sigma}(t) = \int_{S^2} [\boldsymbol{\Sigma}_n](\boldsymbol{p}, t)\, \psi(\boldsymbol{p}, t)\, \mathrm{d}\Omega = N \langle [\boldsymbol{\Sigma}_n] \rangle, \tag{3.30}$$

(recall the definition of the orientational average in (3.6)). Thus, defining the volume fraction $\phi = N(\pi a^2 L)/V$, we find the leading order contribution to the effective stress in ϕ to be

$$\boldsymbol{\Sigma} = \frac{\mu\phi}{3\varepsilon^2(c+2)} \left(\langle \boldsymbol{pppp} \rangle - \frac{1}{3}\mathbf{I}\langle \boldsymbol{pp} \rangle \right) : \mathbf{E}^\infty. \tag{3.31}$$

Should we be concerned that this extra stress scales as $\phi/(\varepsilon^2 \log(\varepsilon))$? This just means that ϕ has to be much smaller than $|\varepsilon^2 \log(\varepsilon)|$ in order for this theory to apply. But this is not unreasonable, since rods will affect each other through the fluid not when they are a distance $\sim \varepsilon$ from each other, but instead when they are a distance $\sim L$ from each other. Defining instead $\Phi := N(4\pi(L/2)^3/3)/V$, which is close to 1 when the spheres swept out by each rod, spinning randomly about their centers, are becoming close packed, then

$$\boldsymbol{\Sigma} = \frac{2\mu\Phi}{(c+2)} \left(\langle \boldsymbol{pppp} \rangle - \frac{1}{3}\mathbf{I}\langle \boldsymbol{pp} \rangle \right) : \mathbf{E}^\infty. \tag{3.32}$$

Welp, I guess we need to know about the particle statistics to say more.

3.4 Equilibrium distributions with no flow: Boltzmann to Bingham

So we have the extra stress, in (3.32). Kind of. We can compute it for a given distribution, ψ. But ψ is also changing in time due to the background flow. So we need to incorporate the dynamics of ψ, which brings us back to the continuity equation, or if we include Brownian fluctuations, the Smoluchowski equation (3.5). The rotational diffusivity, d, comes from the Stokes-Einstein relation, which balances the viscous energy cost for particle rotation and the thermal energy driving the fluctuations (see Graham (2018)), leading to $d = k_B T/\zeta_r$, where k_B is Boltzmann's constant and T is the temperature, and ζ_r is the rotational drag defined in (3.24).

Let's study the equilibrium of (3.5) (for which $\psi_t = 0$), first with no imposed background flow. Then $d\nabla_{\boldsymbol{p}}^2 \psi = 0$, so $\psi = N/(4\pi)$, constant. This is the isotropic distribution. Nothing in the system is promoting any order. It is also interesting to consider additional physics, not hydrodynamic in origin. For instance, the particles may experience an aligning potential $U(\boldsymbol{p})$, from an external field, or a mean-field interaction, so that (with no background flow) $\zeta_r \dot{\boldsymbol{p}} = -\nabla_{\boldsymbol{p}} U$. The distribution at equilibrium is a balance between this alignment and rotational diffusivity (a zero flux condition):

$$\nabla_{\boldsymbol{p}} \cdot (\dot{\boldsymbol{p}}\psi) = d\nabla_{\boldsymbol{p}}^2 \psi \tag{3.33}$$

$$\Rightarrow -(\nabla_{\boldsymbol{p}} U)\psi - k_B T \nabla_{\boldsymbol{p}} \psi = 0 \tag{3.34}$$

$$\Rightarrow (-\nabla_{\boldsymbol{p}} U - k_B T \nabla_{\boldsymbol{p}} \log(\psi))\, \psi = 0 \tag{3.35}$$

$$\Rightarrow -\nabla_{\boldsymbol{p}} U - k_B T \nabla_{\boldsymbol{p}} \log(\psi) = 0 \tag{3.36}$$

$$\Rightarrow \log(\psi) = \frac{-U(\boldsymbol{p})}{k_B T} + \text{const.}, \tag{3.37}$$

or

$$\psi = \frac{1}{Z} \exp\left(-U(\boldsymbol{p})/k_B T\right), \tag{3.38}$$

where Z is a normalization constant, found using (3.4). This is called the Boltzmann distribution, or a Gibbs distribution. For a quadratic potential, $U = -\frac{1}{2}\,\boldsymbol{pp} : \mathbf{B}'$, we have

$$\psi = \frac{1}{Z}\exp\left(\boldsymbol{pp} : \mathbf{B}\right), \tag{3.39}$$

where $\mathbf{B} = \mathbf{B}'/(2k_BT)$. The above is called the Bingham distribution (see Bingham (1974)), which is similar to a Gaussian but is confined to the unit sphere, $\boldsymbol{p} \in S^2$. We are starting to sneak up on liquid crystal theories, but that is for another time and/or lecturer.

3.5 Suspension rheology and shear thinning

Among the most important flows to probe a fluid's rheology, or response to deformation, is a steady shear flow. It is easy to imagine a related experiment, shearing a fluid filled with a small concentration of rodlike bodies between two plates, and measuring the forces it takes to do so. Plate-plate and cone-plate rheometers classically perform exactly this test in a rotational geometry. Let's see what we should expect to find.

Consider a steady shear flow, $\boldsymbol{u}^\infty = \dot{\gamma} y\hat{\boldsymbol{x}}$, so that $\mathbf{A}^\infty = \dot{\gamma}\,\hat{\boldsymbol{y}}\hat{\boldsymbol{x}}$, $\mathbf{E}^\infty = \frac{\dot{\gamma}}{2}(\hat{\boldsymbol{y}}\hat{\boldsymbol{x}} + \hat{\boldsymbol{x}}\hat{\boldsymbol{y}})$, $\mathbf{W}^\infty = \frac{\dot{\gamma}}{2}(\hat{\boldsymbol{y}}\hat{\boldsymbol{x}} - \hat{\boldsymbol{x}}\hat{\boldsymbol{y}})$, and $\boldsymbol{\omega}^\infty = \nabla \times \boldsymbol{u}^\infty = -\dot{\gamma}\hat{\boldsymbol{z}}$, where $\hat{\boldsymbol{z}} = \hat{\boldsymbol{x}} \times \hat{\boldsymbol{y}}$, so that, from (3.22), we have

$$\dot{\boldsymbol{p}} = \frac{\dot{\gamma}}{2}\left[-\hat{\boldsymbol{z}} \times \boldsymbol{p} + (\mathbf{I} - \boldsymbol{pp}) \cdot (\boldsymbol{p} \cdot (\hat{\boldsymbol{x}}\hat{\boldsymbol{y}} + \hat{\boldsymbol{y}}\hat{\boldsymbol{x}}))\right]. \tag{3.40}$$

We can see a problem right away, if the rod is initially in the shear plane. Writing $\boldsymbol{p} = \cos\theta(t)\hat{\boldsymbol{x}} + \sin\theta(t)\hat{\boldsymbol{y}}$, then the above gives $\dot{\theta} = -\dot{\gamma}\sin^2(\theta)$. A rod will rotate until it asymptotically approaches either $\theta = 0$ or $\theta = \pi$, and that's the end of it! That is exactly the kind of issue that will destroy an attempt to compute a statistical average. Here again, some rotational diffusivity is enough to regularize the distribution, so that $\boldsymbol{p}$ explores all of the possible configuration space.

After a transient startup period, we seek a steady distribution ψ that balances the aligning action of the flow against rotational diffusion, which satisfies

$$\nabla_{\boldsymbol{p}} \cdot (\dot{\boldsymbol{p}}\,\psi) = d\,\nabla_{\boldsymbol{p}}^2\psi. \tag{3.41}$$

This is now much harder to work with than in the previous section, since $\dot{\boldsymbol{p}}$ cannot be written as a gradient flow. So, we seek a small parameter. To this end, we define the dimensionless rotational Péclet number, $\mathrm{Pe} = \dot{\gamma}/d$, which compares the aligning effect of the background shear flow to the rotational diffusivity; the latter drives the distribution back towards isotropy.

Let's investigate some limiting behaviors. When $\mathrm{Pe} = 0$, we have the isotropic distribution from before, $\psi = N/(4\pi)$. The rods still contribute to the effective viscosity, but we end up with a quasi-Newtonian fluid again. The quantities needed for (3.32) are:

$$\langle \boldsymbol{pp} \rangle = \frac{1}{N}\int_{S^2} \boldsymbol{pp}\left(\frac{N}{4\pi}\right) d\Omega = \frac{1}{3}\mathbf{I}, \tag{3.42}$$

$$\langle p_i p_j p_k p_\ell \rangle = \tfrac{1}{15}(\delta_{ij}\delta_{k\ell} + \delta_{ik}\delta_{j\ell} + \delta_{i\ell}\delta_{jk}), \tag{3.43}$$

(see Exercise 3.4) and so the *hydrodynamic* part of the extra stress $\boldsymbol{\Sigma}$ for an isotropic distribution is $\boldsymbol{\Sigma}^H = 2\mu'_H\,\mathbf{E}^\infty$, where

$$\mu'_H = \frac{2\mu\Phi}{15(c+2)}. \tag{3.44}$$

For small but non-zero Péclet number, Leal and Hinch (1971) and Hinch and Leal (1972) (following Giesekus, 1962) carried out an expansion in small Pe, writing $\psi = \frac{N}{4\pi}(1 + \mathrm{Pe}\,\psi_1 + \mathrm{Pe}^2\psi_2 + \cdots)$, and solving the steady Smoluchowski equation order by order. At first order, they found that

$$\psi_1 = \tfrac{1}{2}\,\boldsymbol{pp} : \hat{\mathbf{E}}^\infty, \tag{3.45}$$

where $\hat{\mathbf{E}}^\infty = \mathbf{E}^\infty/\dot{\gamma}$ is dimensionless. (How, exactly? You'll do the calculation in Exercise 3.6, though only in two dimensions). So, the first effect of the flow is to promote an alignment of the rods along the extensional axis of the shear (at a 45° angle relative to the flow direction). But the effect on the viscosity is not registered at this order in Pe, can you guess why? We would expect an extra viscosity (which is specific to this shear flow, mind you!) of $\mu_0'(1 + c_1\mathrm{Pe} + c_2\mathrm{Pe}^2 + ...)$. Would you agree that reversing the flow direction should not affect the steady effective viscosity? Well that would take $\mathrm{Pe} \to -\mathrm{Pe}$, and then the effective viscosity would be $\mu_0'(1-c_1\mathrm{Pe}+c_2\mathrm{Pe}^2+...)$. So it must be that $c_1 = 0$. On symmetry grounds alone, the effective viscosity must be an $O(\mathrm{Pe}^2)$ effect (or higher).

But at small flow rates there is actually another, larger extra stress that we have not yet discussed: a *Brownian* stress. If the solvent is exerting stresses on the rods, generating Brownian fluctuations, then the rods are generating stresses back on the solvent as well. Using the rotational Stokes-Einstein relation, $\zeta_r d = k_B T$, with ζ_r from (3.24), this stress is found at $O(\mathrm{Pe})$ to be

$$\mathbf{\Sigma}^B = \frac{12\mu\Phi\, d}{c+4}\,\mathbf{Q} = \frac{4\mu\Phi}{5(c+4)}\mathbf{E}^\infty \tag{3.46}$$

(see Exercise 3.9).

Hence, associated with the more aligned distribution for non-zero but small Pe, the limiting viscosity at low shear rates is found to be $\mu_0 = \mu + \mu_0'$, where the extra viscosity is a combination of hydrodynamic and Brownian contributions,

$$\mu_0' = \mu_H' + \mu_B' = \frac{2\mu\Phi}{15(c+2)} + \frac{2\mu\Phi}{5(c+4)}. \tag{3.47}$$

Hinch and Leal (1972) then continued on to second order in Pe (see also Brenner (1974); Doi and Edwards (1986); Graham (2018)), and found $c_2 < 0$. So the extra viscosity actually diminishes for increased flow rates. This fluid is 'shear thinning': when the fluid is sheared rapidly, the registered viscosity of the fluid is lower than when it is not sheared (or sheared very slowly). This is because the rods are, on average, becoming more aligned with the flow direction, and a rod aligned with the flow direction has $\boldsymbol{pp} : \mathbf{E}^\infty \to 0$ (no stresslet is exerted on the flow by the particle).

At yet higher shear rates, the mean rod orientation dips even closer to the axis of the flow direction, where the rods reside longest (recall $\dot{\theta} \sim -\dot{\gamma}\sin^2\theta$ near $\theta = 0$, with diffusion needed to nudge the rod past that barrier). The high Pe limit is singular, so the asymptotics are more interesting; they predict an extra viscosity $\sim \mathrm{Pe}^{-1/3}$ as $\mathrm{Pe} \to \infty$, vanishing entirely as the rods all become (on average) perfectly aligned with the background flow.

In summary, the effective viscosity for this shear flow experiment is immediately larger than that of the solvent alone, encoded by the zero shear viscosity, $\mu_0 = \mu(1 + \frac{2\Phi}{15(c+2)} + \frac{2\Phi}{5(c+4)})$, but the effective viscosity diminishes as the shear rate is increased, reducing all the way down to simply $\mu_\infty = \mu$ at very large shear rates. ('Normal stress differences' remain, however, at $\mathrm{Pe} \to \infty$, due to the fluid anisotropy. This results in an effective fluid elasticity. We'll come back to this in the next lecture.)

3.6 The closure problem

In general, we have that the extra stress, $\mathbf{\Sigma}$, depends on the particle distribution, ψ, via the averages $\langle \boldsymbol{pppp} \rangle$ and $\langle \boldsymbol{pp} \rangle$. It would be particularly helpful to simply write evolution equations for these tensors directly. To see how that would go, notice what happens when we multiply the Smoluchowski equation, (3.5), by $\boldsymbol{pp}$, and integrate:

$$\int_{S^2} \boldsymbol{pp}\,\psi_t\,\mathrm{d}\Omega + \int_{S^2} \boldsymbol{pp}\,\nabla_{\boldsymbol{p}} \cdot (\dot{\boldsymbol{p}}\psi)\,\mathrm{d}\Omega = d\int_{S^2} \boldsymbol{pp}\,\nabla_{\boldsymbol{p}}^2\psi\,\mathrm{d}\Omega. \tag{3.48}$$

Extracting the time derivative from the first integrand, the first term is just $N\dot{\mathbf{M}}$, where $\mathbf{M} = \langle \boldsymbol{pp} \rangle$ is the second orientational moment. Integrating the other two terms by parts (see Exercise 3.8), we find that

$$\dot{\mathbf{M}} = \mathbf{E}^\infty \cdot \mathbf{M} + \mathbf{M} \cdot \mathbf{E}^\infty + \mathbf{M} \cdot \mathbf{W}^\infty - \mathbf{W}^\infty \cdot \mathbf{M} - 2 \langle \boldsymbol{pppp} \rangle : \mathbf{E}^\infty - 6d \left(\mathbf{M} - \tfrac{1}{3}\mathbf{I} \right). \tag{3.49}$$

And, inserting the definitions of $\mathbf{E}$ and $\mathbf{W}$, note that (for a generic matrix $\mathbf{M}$),

$$\mathbf{E} \cdot \mathbf{M} + \mathbf{M} \cdot \mathbf{E} + \mathbf{M} \cdot \mathbf{W} - \mathbf{W} \cdot \mathbf{M} = \nabla \boldsymbol{u}^T \cdot \mathbf{M} + \mathbf{M} \cdot \nabla \boldsymbol{u}. \tag{3.50}$$

This is the 'co-deformational' part of the time rate of change of $\mathbf{M}$, it corresponds to the deformation of the basis vectors representing the second orientational moment, $\mathbf{M}$, under the action of the linear flow. We will return to this object again in the third lecture.

Equivalently, using $\mathbf{Q} = \mathbf{M} - \frac{1}{3}\mathbf{I}$ (and $\dot{\mathbf{Q}} = \dot{\mathbf{M}}$), we find that

$$\dot{\mathbf{Q}} - (\nabla \boldsymbol{u}^\infty)^T \cdot \mathbf{Q} - \mathbf{Q} \cdot \nabla \boldsymbol{u}^\infty = \tfrac{2}{3}\mathbf{E}^\infty - 2 \langle \boldsymbol{pppp} \rangle : \mathbf{E}^\infty - 6d\, \mathbf{Q}. \tag{3.51}$$

We see that rotational diffusivity drives the system back towards isotropy ($-6d\,\mathbf{Q}$ drives $\mathbf{Q} \to \mathbf{0}$). But now it appears that we need an equation for the fourth moment, $\langle \boldsymbol{pppp} \rangle$. Sadly, when we seek out such an evolution equation we find that it depends on the sixth moment, and the sixth moment depends on the eighth, and so on. The equations for the moments are not 'closed'. So either we can solve the full (3.5) (which nowadays is quite possible numerically using the most advanced tools), or a closure approximation must be selected.

A classical, severe truncation is the Doi closure (Doi, 1981), $\langle \boldsymbol{pppp} \rangle \approx \langle \boldsymbol{pp} \rangle \langle \boldsymbol{pp} \rangle$. When is this a sensible approximation? This is exact when $\psi = \delta(\boldsymbol{p} - \boldsymbol{p}_0)$, i.e. every rod is pointed in the same direction, $\boldsymbol{p}_0$. (Since the rods are fore-aft symmetric, the distribution should be as well, so really we should write $\psi = (\delta(\boldsymbol{p} - \boldsymbol{p}_0) + \delta(\boldsymbol{p} + \boldsymbol{p}_0))/2$, and get the same result. See Exercise 3.7) It will be a good approximation when the suspension is closer to being aligned, and it will not be a very good approximation when the distribution is closer to isotropic.

Inserting the Doi closure eliminates the fourth moment in (3.51), since $\langle \boldsymbol{pppp} \rangle : \mathbf{E}^\infty \approx \mathbf{M}\,(\mathbf{M} : \mathbf{E}^\infty) = (\mathbf{Q} : \mathbf{E}^\infty)(\mathbf{Q} + \frac{1}{3}\mathbf{I})$ (use Exercise 3.4). The Stokes equations, together with the extra stress (3.32), now represent a closed system for the velocity $\boldsymbol{u}$ and the order parameter $\mathbf{Q}$:

$$-\nabla p + \mu \nabla^2 \boldsymbol{u} + \nabla \cdot \boldsymbol{\Sigma} = \mathbf{0}, \tag{3.52}$$

$$\boldsymbol{\Sigma} = \frac{2\mu\Phi}{c+2} \left(\mathbf{Q} : \mathbf{E}^\infty \right) \mathbf{Q}, \tag{3.53}$$

$$\dot{\mathbf{Q}} - (\nabla \boldsymbol{u}^\infty)^T \cdot \mathbf{Q} - \mathbf{Q} \cdot \nabla \boldsymbol{u}^\infty = \tfrac{2}{3}\mathbf{E}^\infty - 2\,(\mathbf{Q} : \mathbf{E}^\infty)(\mathbf{Q} + \tfrac{1}{3}\mathbf{I}) - 6d\,\mathbf{Q}, \tag{3.54}$$

$$\nabla \cdot \boldsymbol{u} = 0. \tag{3.55}$$

Voilà! We no longer need to solve (3.5), we can just solve the system above. But note that at isotropy, where $\mathbf{Q} = \mathbf{0}$, we have $\boldsymbol{\Sigma} = \mathbf{0}$, which we know is wrong (we didn't reproduce the zero shear viscosity, for instance). That mistake is consistent with the inaccuracy of the Doi closure when the suspension is not nearly aligned. So the system above should be more accurate for settings with substantial flow rates.

To improve the accuracy of this approach, other closures were invented. One idea was to carefully interpolate between asymptotic expansions near the isotropic and highly aligned limits (Hinch and Leal, 1976). Another closure is called the Bingham closure, in which one approximates ψ locally by a Bingham distribution (3.39) whose parameters are fixed by the current $\mathbf{Q}$, and evaluates $\langle \boldsymbol{pppp} \rangle$ from that fit; this closure is also constructed to be exact in both the isotropic and perfectly-aligned limits (Chaubal and Leal, 1998). For an example of this closure applied to active suspensions, see Weady et al. (2022).

3.7 The Carreau-Yasuda and power-law models

As a final note, the kinetic theory approach above is very appealing, in that all terms and coefficients appearing in the moment equations (the equations for macroscopic variables) are well motivated from microscopic first principles. But when a suspension is non-dilute, the situation is far more complicated, and it is common to pursue an empirical modeling approach. In this approach, the macroscopic quantities are taken to be the fundamental building blocks, and the equations describing them incorporate symmetries known to exist in the system.

Among models of this type, the simplest departure from Newtonian behavior keeps the stress local, instantaneous, and aligned with the rate of strain, but lets the viscosity depend on the local shear rate. In a *generalized Newtonian fluid*, the deviatoric stress is written as

$$\boldsymbol{\tau} = \mu(\dot{\gamma})\,\dot{\boldsymbol{\gamma}}, \qquad \dot{\boldsymbol{\gamma}} := \nabla \boldsymbol{u} + (\nabla \boldsymbol{u})^T = 2\mathbf{E}, \qquad \dot{\gamma} := \sqrt{\tfrac{1}{2}\,\dot{\boldsymbol{\gamma}} : \dot{\boldsymbol{\gamma}}} = \sqrt{2\,\mathbf{E} : \mathbf{E}}, \tag{3.56}$$

where $\dot{\gamma}$ is the scalar shear rate (the second invariant of the rate-of-strain). Another popular empirical form is the *Carreau-Yasuda* model,

$$\mu(\dot{\gamma}) = \mu_\infty + (\mu_0 - \mu_\infty)\big[\,1 + (\lambda\dot{\gamma})^a\,\big]^{\frac{n-1}{a}}, \tag{3.57}$$

which interpolates between a zero-shear viscosity μ_0 (for $\dot{\gamma} \ll \lambda^{-1}$) and an infinite-shear viscosity $\mu_\infty < \mu_0$ (for $\dot{\gamma} \gg \lambda^{-1}$), where λ is a relaxation time. The power-law index n controls the degree of shear thinning (or thickening), and a tunes the sharpness of the transition. For relatively large shear rates, or long relaxation times, $\lambda\dot{\gamma} \gg 1$, this reduces to the *power-law* model,

$$\mu(\dot{\gamma}) = K\,\dot{\gamma}^{\,n-1}, \tag{3.58}$$

with consistency index K. For $n = 1$, $K = \mu$ and we recover a Newtonian fluid. If $n < 1$ the fluid is shear-thinning, and for $n > 1$ the fluid is shear-thickening.

We can start to see the relationship of this empirical model to the rod suspension of the previous sections. The kinetic theory derived a similar result from first principles: the viscosity reduced from the zero-shear limit, μ_0 (the hydrodynamic and Brownian value computed previously), to a limiting value as $\mathrm{Pe} \to \infty$. A relaxation timescale for the suspension is given by rotational diffusivity, $\lambda \sim 1/d$. And we expect a shear-thinning transition at $\mathrm{Pe} \sim 1$, when flow alignment and diffusive relaxation timescales are commensurate.

So can we just abandon all the details in the previous section and just use a simple model like a power-law fluid? Perhaps. But there is no free lunch; these models fail to capture the normal-stress differences, which are known to exist, and which are captured in the more complete model of the previous section. Even in the dilute setting, capturing all of the complex fluid mechanical properties at all flow rates is a serious challenge!

Exercise 3.1. Derive the vector identity $\boldsymbol{p} \times (\boldsymbol{\Omega} \times \boldsymbol{p}) = (\mathbf{I} - \boldsymbol{pp}) \cdot \boldsymbol{\Omega}$ using index notation, and show that $\boldsymbol{p} \times (\boldsymbol{\Omega} \times \boldsymbol{p}) = \boldsymbol{\Omega}^\perp$. Then verify (3.22).

Exercise 3.2. Derive the rotational drag coefficient, (3.24). You'll need to revisit (3.17), instead setting $\boldsymbol{L}_v = -\boldsymbol{L}^\perp$, and then revisit (3.18), removing the background flow.

Exercise 3.3. Verify that (3.40) returns $\dot{\theta} = -\dot{\gamma}\sin^2\theta$ for two-dimensional motion confined to the shear plane.

Exercise 3.4. Use symmetry and isotropy arguments to show that $\int_{S^2} \boldsymbol{p}\,d\Omega = \mathbf{0}$, $\int_{S^2} \boldsymbol{pp}\,d\Omega = \frac{4\pi}{3}\mathbf{I}$, $\int_{S^2} \boldsymbol{ppp}\,d\Omega = \mathbf{0}$, and $\int_{S^2} p_i p_j p_k p_\ell\,d\Omega = \frac{4\pi}{15}(\delta_{ij}\delta_{k\ell} + \delta_{ik}\delta_{j\ell} + \delta_{i\ell}\delta_{jk})$. Hint: try $\boldsymbol{p} \to -\boldsymbol{p}$ for the first and third integrals. For the second, note that the result has no sense of direction (isotropy, so it must be the case that $\int_{S^2} p_i p_j\,d\Omega = q\delta_{ij}$), and take a trace. For the fourth, isotropy and symmetry demand that $\int_{S^2} p_i p_j p_k p_\ell\,d\Omega = q(\delta_{ij}\delta_{k\ell} + \delta_{ik}\delta_{j\ell} + \delta_{i\ell}\delta_{jk})$, then contract (double dot product) with $\mathbf{I}$.

Exercise 3.5. Derive the coefficients (3 and 15/2) in (3.7). (Integrate ψ, $\boldsymbol{p}\psi$, and $[\boldsymbol{pp}]\psi$ over the unit sphere, and require orthogonality). Use the results of Exercise 3.4. Note that $\mathbf{M}$ is symmetric.

Exercise 3.6. Consider a suspension which is confined to two spatial dimensions. Perhaps we are studying a very thin film of fluid, relative to the length scale of the rods. Then we can write $\boldsymbol{p} = \cos\theta\hat{\boldsymbol{x}} + \sin\theta\hat{\boldsymbol{y}}$, and the distribution function as $\psi = \psi(\theta, t)$.

1. The Smoluchowski equation, (3.5), is now expressed as $\psi_t + \partial_\theta(\dot{\theta}\psi) = d\psi_{\theta\theta}$. For a planar extensional flow, $\boldsymbol{u}^\infty = \dot{\varepsilon}(x\,\hat{\boldsymbol{x}} - y\,\hat{\boldsymbol{y}})$, use (3.22) to show that $\dot{\theta} = -\dot{\varepsilon}\sin(2\theta)$.

2. Now solve for the equilibrium distribution, where $\psi_t = 0$, and plot the result as a function of the Péclet number, defined for this problem as $\mathrm{Pe} = \dot{\varepsilon}/d$. This is a periodic version of a Gaussian, it is a Bingham distribution! It is also called a von Mises distribution.

3. Find the parameter tensor $\mathbf{B}$ in (3.39) (the matrix in the Bingham distribution) for the equilibrium distribution above.

4. If you seek the steady distribution for a shear flow ($\boldsymbol{u} = \dot{\gamma}y\hat{\boldsymbol{x}}$, $\dot{\theta} = -\dot{\gamma}\sin^2\theta$), there is a wrinkle. Writing $\mathrm{Pe} = \dot{\gamma}/d$, and integrating $\mathrm{Pe}\partial_\theta(\dot{\theta}\psi) = \psi_{\theta\theta}$, once, we have $\mathrm{Pe}\dot{\theta}\psi = \psi_\theta + J$. In the straining flow we could take $J = 0$ and arrive at a periodic solution. Show that there is now no periodic solution if $J = 0$. This system does not exhibit 'detailed balance', meaning that the probability flux (J) is not zero in the steady state. Why not?

Exercise 3.7. Verify that $\langle \boldsymbol{pppp}\rangle \approx \langle \boldsymbol{pp}\rangle\langle \boldsymbol{pp}\rangle$ is exact in the limit that $\psi \to N\delta(\boldsymbol{p} - \boldsymbol{p}_0)$, where $\int_{S^2}\delta(\boldsymbol{p} - \boldsymbol{p}_0)\,d\Omega = 1$, or $\psi \to N(\delta(\boldsymbol{p} - \boldsymbol{p}_0) + \delta(\boldsymbol{p} + \boldsymbol{p}_0))/2$. Show that $\langle \boldsymbol{pp}\rangle\langle \boldsymbol{pp}\rangle : \mathbf{A}$ is not a perfect approximation to $\langle \boldsymbol{pppp}\rangle : \mathbf{A}$ for generic matrix $\mathbf{A}$ when $\psi = N/(4\pi)$ (isotropic), and is a very bad approximation when $\mathrm{tr}(\mathbf{A}) = 0$, for instance if $\mathbf{A} = \mathbf{E}^\infty$.

Exercise 3.8. Derive the second-moment equation (3.49) from (3.48) by verifying the identities below. At some point you'll need to use that $\dot{\boldsymbol{p}} = \boldsymbol{p}\cdot\mathbf{W}^\infty + (\mathbf{I} - \boldsymbol{pp})\cdot(\boldsymbol{p}\cdot\mathbf{E}^\infty)$, and with $\mathbf{M} = \langle \boldsymbol{pp}\rangle$,

$$\dot{\boldsymbol{p}}\cdot\nabla_{\boldsymbol{p}}(\boldsymbol{pp}) = \dot{\boldsymbol{p}}\,\boldsymbol{p} + \boldsymbol{p}\,\dot{\boldsymbol{p}}, \tag{3.59}$$

$$\int_{S^2}\boldsymbol{pp}\,\nabla_{\boldsymbol{p}}\cdot(\dot{\boldsymbol{p}}\,\psi)\,d\Omega = -N\langle \dot{\boldsymbol{p}}\boldsymbol{p} + \boldsymbol{p}\dot{\boldsymbol{p}}\rangle, \tag{3.60}$$

$$\nabla^2_{\boldsymbol{p}}(\boldsymbol{pp}) = 2(\mathbf{I} - 3\boldsymbol{pp}), \tag{3.61}$$

$$\int_{S^2}\boldsymbol{pp}\,\nabla^2_{\boldsymbol{p}}\,\psi\,d\Omega = 2N(\mathbf{I} - 3\mathbf{M}), \tag{3.62}$$

$$\langle \dot{\boldsymbol{p}}\,\boldsymbol{p} + \boldsymbol{p}\,\dot{\boldsymbol{p}}\rangle = \mathbf{E}^\infty\cdot\mathbf{M} + \mathbf{M}\cdot\mathbf{E}^\infty + \mathbf{M}\cdot\mathbf{W}^\infty - \mathbf{W}^\infty\cdot\mathbf{M} - 2\langle \boldsymbol{pppp}\rangle : \mathbf{E}^\infty. \tag{3.63}$$

Then quickly verify that $\mathbf{E}^\infty\cdot\mathbf{M} + \mathbf{M}\cdot\mathbf{E}^\infty + \mathbf{M}\cdot\mathbf{W}^\infty - \mathbf{W}^\infty\cdot\mathbf{M} = (\nabla\boldsymbol{u}^\infty)^T\cdot\mathbf{M} + \mathbf{M}\cdot\nabla\boldsymbol{u}^\infty$.

Exercise 3.9. Extra credit. Verify (3.46). Hint: Use (3.45) to compute (3.32), and the results of Exercise 3.4. Note that all particles are assumed to experience the same background flow, in this representative volume element.

4 Lecture 3: From Hookean Dumbbells to Oldroyd-B and Active Suspensions

In the previous lecture we studied a dilute suspension of rigid rods. One of the challenges of that system is that $\boldsymbol{p}$ resides on the unit sphere. In this lecture, we are going to visit a similar system, a suspension of Hookean dumbbells, which model more complex but real elongated polymers. And we will enjoy a more dramatic example of viscoelasticity. Finally, we will touch upon active suspensions, and the undiscovered country represented by active suspensions in complex fluids.

4.1 From rods to Hookean dumbbells

We will once again assume a well-mixed, dilute suspension, so that the concentration of particles is assumed to be uniform in space. Then the particle number density is only a function of the state variable, $\boldsymbol{R}$, and time, t, $\psi(\boldsymbol{R}, t)$, normalized so that $N = \int_{\mathbb{R}^3} \psi \, \mathrm{d}v$ is the number of dumbbells, and per-particle averages read $\langle \boldsymbol{q} \rangle = \frac{1}{N} \int_{\mathbb{R}^3} \boldsymbol{q} \, \psi \, \mathrm{d}v$, just as in (3.6). Some of the names have changed: instead of the second orientational moment being the nematic order parameter, we now call $\mathbf{M} = \langle \boldsymbol{RR} \rangle$ the conformation tensor. Everything we covered in the second lecture follows, but the fact that $\boldsymbol{R} \in \mathbb{R}^3$ is an improvement. The Smoluchowski equation still reads as

$$\psi_t + \nabla_{\boldsymbol{R}} \cdot (\dot{\boldsymbol{R}} \, \psi) = d \nabla^2_{\boldsymbol{R}} \psi, \tag{4.1}$$

but now we have a simpler gradient operator, $\nabla_{\boldsymbol{R}} = \partial / \partial \boldsymbol{R}$. Integration by parts is going to be a breeze!

First, what is $\dot{\boldsymbol{R}}$? As a simple model, we treat the dumbbell as two spherical beads of radius a, separated by the end-to-end vector $\boldsymbol{R}$, connected by a spring which exerts a force $\boldsymbol{F}_s = K\boldsymbol{R}$. The viscous drag on each bead, neglecting their hydrodynamic interactions, is proportional to the difference between the flow at the bead center and its velocity (the Faxén law, from (2.19)), and we define the resistance coefficient as $\zeta = 6\pi\mu a$. The nth dumbbell contributes the force dipole $V\boldsymbol{\Sigma}_{el} = K\boldsymbol{RR}$; summing over the N dumbbells and once again tucking the isotropic part into the pressure, gives an extra elastic stress,

$$\boldsymbol{\Sigma} = \sum_{n=1}^{N} [\boldsymbol{\Sigma}_{el}] = \frac{NK}{V} \Big(\mathbf{M} - \tfrac{1}{3} \mathrm{tr}(\mathbf{M}) \, \mathbf{I} \Big). \tag{4.2}$$

This is the Kramers form of the polymer stress (Bird et al., 1987), here recovered by evaluating Batchelor's formula applied to the two spheres of the dumbbell. Great! But now again we need the dynamics of $\mathbf{M}$ to close the system.

Multiplying (4.1) by $\boldsymbol{RR}$ and integrating by parts, using $\int \boldsymbol{RR} \, \nabla_{\boldsymbol{R}} \cdot (\boldsymbol{R} \cdot \mathbf{A} \, \psi) \, \mathrm{d}^3 R = -N \left(\mathbf{A}^T \cdot \langle \boldsymbol{RR} \rangle - \langle \boldsymbol{RR} \rangle \cdot \mathbf{A} \right)$ and $\int \boldsymbol{RR} \, \nabla_{\boldsymbol{R}} \cdot (\nabla_{\boldsymbol{R}} \psi) \, \mathrm{d}^3 R = 2N\mathbf{I}$ (like in Exercise 3.8, but easier), this time we actually get a *closed* evolution equation for the conformation tensor! Using $\langle \boldsymbol{RF}_s \rangle = K\mathbf{M}$, we find

$$\overset{\nabla}{\mathbf{M}} = \frac{4k_B T}{\zeta} \, \mathbf{I} - \frac{4}{\zeta} \, \langle \boldsymbol{RF}_s \rangle = \frac{4k_B T}{\zeta} \, \mathbf{I} - \frac{4K}{\zeta} \, \mathbf{M}, \tag{4.3}$$

or

$$\overset{\nabla}{\mathbf{M}} = -\frac{4K}{\zeta} \left(\mathbf{M} - \mathbf{M}_{eq} \right), \tag{4.4}$$

where $\mathbf{M}_{eq} = (k_B T / K)\mathbf{I}$ is an equilibrium, and we have defined a new time derivative:

$$\overset{\nabla}{\mathbf{A}} := \partial_t \mathbf{A} + \boldsymbol{u} \cdot \nabla \mathbf{A} - \nabla \boldsymbol{u}^T \cdot \mathbf{A} - \mathbf{A} \cdot \nabla \boldsymbol{u}. \tag{4.5}$$

This is the 'upper-convected' time derivative. It is like the material derivative, $\mathrm{D}/\mathrm{D}t$, in that it is a time derivative in a moving frame; but for tensors, the basis vectors used to represent the tensor can also deform in a flow. Without such a correction, the equations of motion will not be 'objective', meaning that they will differ depending on which mathematical frame is used to represent the fluid, which is not physical (see the example below.) There are other adjustments which render a time derivative objective (the lower-convected time derivative, and a blend of the two, called the Jaumann derivative), but (4.5) is the one we got directly for the conformation tensor using the Smoluchowski equation above.

Solving (4.4) for $\mathbf{M}$ and inserting into (4.2), and using $\overset{\nabla}{\mathbf{M}}_{eq} = \frac{k_B T}{K} \overset{\nabla}{\mathbf{I}} = -(2k_B T / K)\mathbf{E}$, the conformation tensor drops out and we are left with a closed evolution equation for the extra stress alone,

$$\boldsymbol{\Sigma} + \lambda \overset{\nabla}{\boldsymbol{\Sigma}} = 2\mu' \mathbf{E}, \tag{4.6}$$

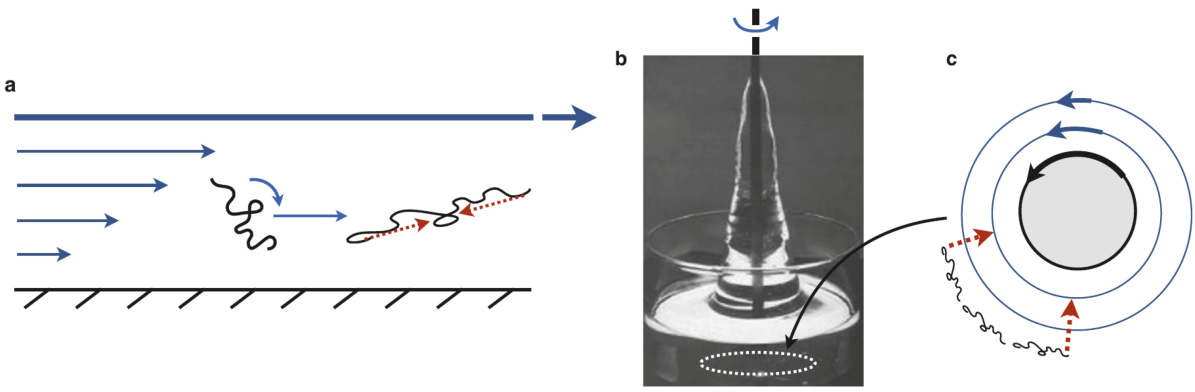

Figure 1: (a) A shear flow rotates and stretches an elongated polymer according to the straining flow, generating anisotropic elastic/particle stresses. (b) The Weissenberg effect (rod climbing): a rod rotated in a viscoelastic fluid drives an upward climb of the free surface, opposite to what is observed in a Newtonian fluid. (c) The effect is explained by normal stress differences: hoop stresses along the curved streamlines 'strangle' the rod, and drive the ascent. Reproduced from Morozov and Spagnolie (2015); the rod-climbing photograph in panel (b) is reproduced from Boger and Walters (1993).

where $\lambda = \zeta/4K$, and $\mu' = \frac{N}{V} k_B T\,\lambda$. A dilute suspension of Hookean dumbbells thus gives what is termed an 'upper-convected Maxwell fluid' or UCM fluid. But having derived this from first (microscopic) principles, rather than measuring or estimating these quantities empirically, the kinetic theory hands us the macroscopic parameters λ, μ' in terms of more specific physical quantities. The kinetic theory approach also helps us better understand how the fluid properties would change as we changed the details of the microstructure.

Instead of the extra particle stress, we could instead write an equation for the total deviatoric stress,

$$\boldsymbol{\tau} = 2\mu \mathbf{E} + \boldsymbol{\Sigma}. \tag{4.7}$$

Written for the total stress, with total viscosity $\eta = \mu + \mu'$ and retardation time $\lambda_r = \lambda\,\mu/(\mu+\mu')$,

$$\boldsymbol{\tau} + \lambda\,\overset{\nabla}{\boldsymbol{\tau}} = 2\eta\Big(\mathbf{E} + \lambda_r\,\overset{\nabla}{\mathbf{E}}\Big). \tag{4.8}$$

This is the Oldroyd-B model fluid[6]. In the solvent-free limit, $\mu \to 0$ ($\lambda_r \to 0$), this collapses back to the UCM model, (4.6). The anisotropic stress carried by the stretched, oriented microstructure can result in very large 'normal stress differences'.

For a shear flow, $\boldsymbol{u} = \dot{\gamma} y \hat{\boldsymbol{x}}$, the first and second normal stress differences are defined as $N_1 = \sigma_{11} - \sigma_{22} = \Psi_1 \dot{\gamma}^2$ and $N_2 = \sigma_{22} - \sigma_{33} = \Psi_2 \dot{\gamma}^2$. These are zero for a Newtonian (or quasi-Newtonian, or even a generalized Newtonian) fluid (see Exercise 4.1). But in viscoelastic fluids they are non-zero (normally, $\Psi_1 > 0$), which results in a strong elastic response to shear. Figure 1 illustrates the dynamics; polymers are aligned and stretched towards the flow direction, building up elastic stresses. The release of such stored elastic energy can drive flows transverse to the flow direction. A striking example of this is found in the kitchen, the Weissenberg 'rod-climbing' effect: in a rotational geometry, such 'hoop stresses' can cause a 'strangulation effect' and fluid is driven towards a central rotating shaft (Fig. 1b-c). This is opposite to what is expected in a Newtonian fluid, where inertia commonly results in a drop in the free surface height near the rod.

[6]The second orientational moment, $\mathbf{M} = \langle \boldsymbol{RR} \rangle$, is a simple enough object, so it must come up everywhere. Here's another place where it pops up. Consider a magnetic field, $\boldsymbol{B}$, then $[\langle \boldsymbol{BB} \rangle]/\mu_0$ is the Maxwell electromagnetic stress tensor (this μ_0 is the permeability of free space). In the large magnetic Reynolds number limit of a MHD (magnetohydrodynamic) flow, there is a perfect mapping onto Oldroyd-B in the large Deborah number limit! See Ogilvie and Proctor (2003).

4.2 Health warning: the linear Maxwell model is not objective

It is tempting to reach the same law with no real effort. The scalar linear Maxwell model for a single spring-dashpot in series (to model the elongated polymer, or dumbbell physics) posits the constitutive law $\sigma + \lambda\dot{\sigma} = \eta\dot{\gamma}$. Naively, we could try to construct a tensor model by promoting the scalars and replacing $\dot{\sigma}$ with a partial time derivative,

$$\boldsymbol{\sigma} + \lambda \frac{\partial}{\partial t}\boldsymbol{\sigma} = \eta\,\dot{\boldsymbol{\gamma}}. \text{ (??)} \tag{4.9}$$

This is wrong: (4.9) is not frame-invariant! Take a look at what happens when you perform an experiment on a train moving at constant velocity $\boldsymbol{u}_0$. The moving-frame stress components are $\sigma_{ij}(\boldsymbol{x} + \boldsymbol{u}_0 t, t)$, whose time derivative

$$\frac{\partial}{\partial t}\sigma_{ij}(\boldsymbol{x} + \boldsymbol{u}_0 t, t) = \frac{\partial \sigma_{ij}}{\partial t} + \boldsymbol{u}_0 \cdot \nabla \sigma_{ij} \tag{4.10}$$

differs from the lab value by $\boldsymbol{u}_0 \cdot \nabla\sigma_{ij}$. But a uniform translation creates no velocity gradients and must not change the stress, so an equation built using $\partial\boldsymbol{\sigma}/\partial t$ like this predicts different physics in the two frames. The cure is a frame-invariant, or *objective*, time derivative, in particular the one we derived naturally in the kinetic theory above. Replacing $\partial/\partial t$ in (4.9) by (4.5) restores frame-invariance and returns precisely the UCM model (4.6). See Morozov and Spagnolie (2015) for more health warnings of this type.

4.3 Active particles

Active particles bring two additional features into the conversation. The first is that they generate additional disturbance flows, whose collective effect (the mean flow) is registered by other particles as additional background flows. This can result in incredibly rich, nonlinear dynamics (Saintillan and Shelley, 2008), a topic which will be covered by other lecturers at this school. The second additional feature is that the particles may themselves be moving on their own through the fluid, as is the case for swimming microorganisms.

The effect of each active particle on the surrounding environment is commonly represented through a multipole representation, as in (2.24). Only the stresslet coefficient contributes to the extra stress in the dilute setting. If the orientation of a uniaxial active particle is denoted by $\boldsymbol{p}$, a common approximation is that the particle swims with velocity $V_s\boldsymbol{p}$, and the symmetric stresslet is denoted by $\mathbf{S} = \alpha\boldsymbol{pp}$, with α an activity strength with units of energy (see Fig. 2). Then, adding up and averaging these contributions to the fluid stress, we have an active stress $\boldsymbol{\Sigma}_a = \frac{N}{V}\langle\alpha(\boldsymbol{pp} - \mathbf{I}/3)\rangle$, so $\boldsymbol{\Sigma}_a = \frac{N}{V}\alpha\mathbf{Q}$, where $\mathbf{Q} = \langle\boldsymbol{pp} - \mathbf{I}/3\rangle$ (N is still the number of particles, and V is still the representative volume element). When $\alpha < 0$ the swimmers are 'pushers', when $\alpha > 0$ they are 'pullers' (see Fig. 2). This results in similar theoretical developments in the dilute limit to those described for suspensions of rods and dumbbells, though an active fluid can explode into intricate dynamics without any coaxing at all from the outside world.

This is a most excellent part of the literature. See Marchetti et al. (2013); Saintillan and Shelley (2015) to take a first step into this area. The effect of activity on the fluid rheology is also very interesting; on this topic, visit the review by Saintillan (2018). But other active flows are of interest as well, including the flows driven by rotating particles, where the leading order hydrodynamic signature of each particle is a 'rotlet'. To get started down that path, see Fruchart et al. (2023); Yeo et al. (2015); Soni et al. (2019).

4.4 Active suspensions in complex fluids

We'll close with a final note, looking ahead to the future. Many aspects of active suspensions in viscous flows are now well understood. And the modeling and examination of bulk complex

fluids is classical. But the dynamics and rheology of active suspensions in complex fluids has barely been explored. In one recent experiment by Liu et al. (2021), microorganisms swimming in a viscoelastic fluid exhibited orientational alignment, classical for active suspensions, but also showed periodic direction reversal, as the fluid periodically gained and released elastic energy!

The space of possibilities is vast. Figure 3 shows one attempt at connecting the many related features of active suspensions and complex fluids, by examining the relationship of the swimmer(s) to the constituents or obstacles that provide the fluid with complex features. Separating distinct regions are the relative lengthscales of the obstacles/swimmers, Bn, the relative relaxation/actuation timescales, De, and the volume fraction of active particles, ϕ. (The theory of individual locomotion through complex fluids, how non-Newtonian rheology reshapes a swimmer's disturbance flow and can modify its gait, is reviewed by Elfring and Lauga (2015); see Sznitman and Arratia (2014) for a parallel discussion of related experimental results.)

The Type-VI octant in Fig. 3 represents this most undiscovered territory, of active matter in complex fluids. Two recent examples are shown in Fig. 4. First shown is theoretical work on a suspension of active particles immersed in a background nematic LC, from Li et al. (2025). Chaotic dynamics at small anchoring strength gives way to a steady, arrested flowing state at large anchoring strengths. See also the work of Lavi et al. (2026).

But swimming is merely a single example of the huge range of activity that biology has to offer. The second example in Fig. 4 shows the growth and division of immotile *E. coli* cells in a nematic LC, which resists bending. The colony remains elongated and is stable to transverse perturbations, leading to giant bacterial chains 200 times longer than an individual cell. Beyond a critical length, the chain buckles. The environment's complex fluid rheology here imbues the immersed biological system with anisotropic, viscoelastic mechanical features. This raises immediate questions about other biological systems, and how they both contribute to and inherit the non-Newtonian mechanics of their surroundings. Active suspensions in complex fluids is a dark and dangerous territory. But rich, and wondrous. Adventurers are needed!

The Road goes ever on and on
Down from the door where it began.
Now far ahead the Road has gone,
And I must follow, if I can,
Pursuing it with eager feet,
Until it joins some larger way
Where many paths and errands meet.
And whither then? I cannot say.

- Bilbo Baggins[7]

Exercise 4.1. Show that in a simple shear flow, $\boldsymbol{u} = \dot{\gamma} y \hat{\boldsymbol{x}}$, the normal stress differences, $N_1 = \sigma_{11} - \sigma_{22}$ and $N_2 = \sigma_{22} - \sigma_{33}$, are zero for a quasi-, generalized-, or just plain old fashioned Newtonian fluid. So any measured normal stress differences in such a flow must be due to non-Newtonian contributions, $N_1 = \Sigma_{11} - \Sigma_{22}$ and $N_2 = \Sigma_{22} - \Sigma_{33}$.

Exercise 4.2. Consider steady simple shear $\boldsymbol{u} = \dot{\gamma}\, y\, \hat{\boldsymbol{x}}$ of an Oldroyd-B fluid (4.8).

1. After a transient period, assume the stress has settled to a steady state, which is independent of x and t (so $\boldsymbol{\Sigma} = \boldsymbol{\Sigma}(y, z)$). Evaluate the upper-convected derivative (4.5) for the stress $\boldsymbol{\Sigma}$, and reduce (4.6) to a linear algebraic system for the components Σ_{ij}.

2. Solve the system to show $\Sigma_{12} = \mu' \dot{\gamma}$, $\Sigma_{11} = 2\mu' \lambda \dot{\gamma}^2$, and $\Sigma_{22} = \Sigma_{33} = 0$.

3. Deduce that the shear viscosity is *constant* (no shear thinning) (i.e. show that $\Sigma_{21} \propto \dot{\gamma}$), while the normal-stress differences are $N_1 = \Sigma_{11} - \Sigma_{22} = 2\mu' \lambda\, \dot{\gamma}^2 > 0$ and $N_2 = \Sigma_{22} - \Sigma_{33} =$

[7] Bilbo appears to have admired Whitman's *Song of the Open Road*.

0, so $\Psi_1 = 2\mu'\lambda$ and $\Psi_2 = 0$ in this model. (Real viscoelastic fluids tend to be shear-thinning, for the reasons described for elongated particles in Lecture 2. So Oldroyd-B is not a perfect model. Life is full of tradeoffs.)

Exercise 4.3. For the same steady shear, solve (4.4) at steady state to find

$$\mathbf{M} = \frac{k_B T}{K} \begin{pmatrix} 1 + 2(\lambda\dot{\gamma})^2 & \lambda\dot{\gamma} & 0 \\ \lambda\dot{\gamma} & 1 & 0 \\ 0 & 0 & 1 \end{pmatrix}. \tag{4.11}$$

Then insert $\mathbf{M}$ into (4.2) to recover the shear stress and normal stress differences in Exercise 4.2.

Exercise 4.4. A UCM fluid (4.6) is sheared steadily and then, at $t = 0$, the flow is switched off ($\boldsymbol{u} = \mathbf{0}$ for $t > 0$). Show that the upper-convected derivative reduces to ∂_t once the flow stops, and hence that every component of the extra stress decays as $\boldsymbol{\Sigma}(t) = \boldsymbol{\Sigma}(0)\, e^{-t/\lambda}$, for a single relaxation time, λ. These are actually fairly simple models! Real viscoelastic fluids can have numerous distinct relaxation times...

References

G. K. Batchelor. The stress system in a suspension of force-free particles. *Journal of Fluid Mechanics*, 41(3):545–570, 1970.

G. K. Batchelor. The effect of Brownian motion on the bulk stress in a suspension of spherical particles. *Journal of Fluid Mechanics*, 83(1):97–117, 1977.

G. K. Batchelor and J. T. Green. The determination of the bulk stress in a suspension of spherical particles to order c^2. *Journal of Fluid Mechanics*, 56(3):401–427, 1972.

C. Bingham. An antipodally symmetric distribution on the sphere. *The Annals of Statistics*, 2 (6):1201–1225, 1974.

R. B. Bird, R. C. Armstrong, and O. Hassager. *Dynamics of Polymeric Liquids, Vol. 1: Fluid Mechanics*. Wiley-Interscience, 2nd edition, 1987.

J. R. Blake. A spherical envelope approach to ciliary propulsion. *Journal of Fluid Mechanics*, 46 (1):199–208, 1971.

D. V. Boger and K. Walters. *Rheological Phenomena in Focus*. Elsevier, Amsterdam, 1993.

H. Brenner. Rheology of a dilute suspension of axisymmetric Brownian particles. *International Journal of Multiphase Flow*, 1(2):195–341, 1974.

T. G. J. Chandler and S. E. Spagnolie. Rigid and deformable bodies in nematic liquid crystals. *Physical Review Fluids*, 9(11):110511, 2024.

C. V. Chaubal and L. G. Leal. A closure approximation for liquid-crystalline polymer models based on parametric density estimation. *Journal of Rheology*, 42(1):177–201, 1998.

A. T. Chwang and T. Y. Wu. Hydromechanics of low-Reynolds-number flow. Part 2. Singularity method for stokes flows. *Journal of Fluid mechanics*, 67(4):787–815, 1975.

P. G. de Gennes and J. Prost. *The Physics of Liquid Crystals*. International Series of Monographs on Physics. Oxford University Press, 2nd edition, 1993.

M. Doi. Molecular dynamics and rheological properties of concentrated solutions of rodlike polymers in isotropic and liquid crystalline phases. *Journal of Polymer Science: Polymer Physics Edition*, 19(2):229–243, 1981.

M. Doi and S. F. Edwards. *The Theory of Polymer Dynamics.* Oxford University Press, 1986.

A. Einstein. Eine neue bestimmung der moleküldimensionen. *Annalen der Physik*, 324(2): 289–306, 1906.

G. J. Elfring and E. Lauga. Theory of locomotion through complex fluids. In *Complex Fluids in Biological Systems*, pages 283–317. Springer, New York, 2015.

M. Fruchart, C. Scheibner, and V. Vitelli. Odd viscosity and odd elasticity. *Annual Review of Condensed Matter Physics*, 14:471–510, 2023.

H. Giesekus. Elasto-viskose flüssigkeiten, für die in stationären schichtströmungen sämtliche normalspannungskomponenten verschieden groß sind. *Rheologica Acta*, 2(1):50–62, 1962.

S. Gonzalez La Corte, T. G. J. Chandler, S. E. Spagnolie, N. S. Wingreen, and S. S. Datta. Morphogenesis of bacterial colonies in liquid crystalline environments. *arXiv preprint arXiv:2512.12406*, 2025.

T. Götz. *Interactions of Fibers and Flow: Asymptotics, Theory and Numerics.* PhD thesis, University of Kaiserslautern, 2000.

Michael D. Graham. *Microhydrodynamics, Brownian Motion, and Complex Fluids.* Cambridge Texts in Applied Mathematics. Cambridge University Press, 2018.

E. Guazzelli and J. F. Morris. *A Physical Introduction to Suspension Dynamics.* Cambridge University Press, 2012.

J. Happel and H. Brenner. *Low Reynolds Number Hydrodynamics.* Martinus Nijhoff, 1983.

E. J. Hinch and L. G. Leal. The effect of Brownian motion on the rheological properties of a suspension of non-spherical particles. *Journal of Fluid Mechanics*, 52(4):683–712, 1972.

E. J. Hinch and L. G. Leal. Constitutive equations in suspension mechanics. Part 2. approximate forms for a suspension of rigid particles affected by Brownian rotations. *Journal of Fluid Mechanics*, 76(1):187–208, 1976.

C. Hohenegger and M. J. Shelley. Dynamics of complex biofluids. In *New Trends in the Physics and Mechanics of Biological Systems.* Oxford University Press, 2011.

G. A. Holzapfel. *Nonlinear Solid Mechanics: A Continuum Approach for Engineering.* John Wiley & Sons, 2000.

T. Ishikawa, M. P. Simmonds, and T. J. Pedley. Hydrodynamic interaction of two swimming model micro-organisms. *Journal of Fluid Mechanics*, 568:119–160, 2006.

G. B. Jeffery. The motion of ellipsoidal particles immersed in a viscous fluid. *Proceedings of the Royal Society A*, 102(715):161–179, 1922.

R. E. Johnson. An improved slender-body theory for Stokes flow. *Journal of Fluid Mechanics*, 99(2):411–431, 1980.

J. B. Keller and S. I. Rubinow. Slender-body theory for slow viscous flow. *Journal of Fluid Mechanics*, 75(4):705–714, 1976.

S. Kim and S. J. Karrila. *Microhydrodynamics: Principles and Selected Applications*. Butterworth-Heinemann, 1991.

L. D. Landau and E. M. Lifshitz. *Fluid Mechanics*. Course of Theoretical Physics, Vol. 6. Pergamon Press, 2nd edition, 1987.

R. G. Larson. *The Structure and Rheology of Complex Fluids*. Oxford University Press, 1999.

I. Lavi, R. Alert, J.-F. Joanny, and J. Casademunt. Dynamical arrest in active nematic turbulence. *Physical Review Research*, 8(1):013294, 2026.

L. G. Leal and E. J. Hinch. The effect of weak Brownian rotations on particles in shear flow. *Journal of Fluid Mechanics*, 46(4):685–703, 1971.

J. Li, L. Ohm, and S. E. Spagnolie. Arrested development and traveling waves of active suspensions in nematic liquid crystals. *Physical Review Fluids*, 10(8):083301, 2025.

S. Liu, S. Shankar, M. C. Marchetti, and Y. Wu. Viscoelastic control of spatiotemporal order in bacterial active matter. *Nature*, 590(7844):80–84, 2021.

M. C. Marchetti, J. F. Joanny, S. Ramaswamy, T. B. Liverpool, J. Prost, Madan Rao, and R. Aditi Simha. Hydrodynamics of soft active matter. *Reviews of Modern Physics*, 85(3): 1143–1189, 2013.

M. R. Maxey and J. J. Riley. Equation of motion for a small rigid sphere in a nonuniform flow. *Physics of Fluids*, 26(4):883–889, 1983.

O. Maxian and A. Donev. Slender body theories for rotating filaments. *Journal of Fluid Mechanics*, 952:A5, 2022.

S. Michelin and E. Lauga. Phoretic self-propulsion at finite péclet numbers. *Journal of Fluid Mechanics*, 747:572–604, 2014.

Y. Mori, L. Ohm, and D. Spirn. Theoretical justification and error analysis for slender body theory with free ends. *Archive for Rational Mechanics and Analysis*, 235(3):1905–1978, 2020.

A. Morozov and S. E. Spagnolie. Introduction to complex fluids. In S. E. Spagnolie, editor, *Complex Fluids in Biological Systems*, pages 3–52. Springer, New York, 2015.

G. I. Ogilvie and M. R. E. Proctor. On the relation between viscoelastic and magnetohydrodynamic flows and their instabilities. *Journal of Fluid Mechanics*, 476:389–409, 2003.

L. Ohm. A free boundary problem for an immersed filament in 3d stokes flow. *arXiv preprint arXiv:2404.04737*, 2024.

O. S. Pak and E. Lauga. Generalized squirming motion of a sphere. *Journal of Engineering Mathematics*, 88(1):1–28, 2014.

G. Peng and O. Schnitzer. Universal square-root-log scaling for slender-body end effects. *arXiv preprint arXiv:2605.24653*, 2026.

D. Saintillan. Rheology of active fluids. *Annual Review of Fluid Mechanics*, 50:563–592, 2018.

D. Saintillan and M. J. Shelley. Instabilities and pattern formation in active particle suspensions: kinetic theory and continuum simulations. *Physical Review Letters*, 100(17):178103, 2008.

D. Saintillan and M. J. Shelley. Theory of active suspensions. In *Complex Fluids in Biological Systems*, pages 319–355. Springer, New York, 2015.

V. Soni, E. S. Bililign, S. Magkiriadou, S. Sacanna, D. Bartolo, M. J. Shelley, and W. T. M. Irvine. The odd free surface flows of a colloidal chiral fluid. *Nature Physics*, 15(11):1188–1194, 2019.

S. E. Spagnolie and E. Lauga. Hydrodynamics of self-propulsion near a boundary: predictions and accuracy of far-field approximations. *Journal of Fluid Mechanics*, 700:105–147, 2012.

S. E. Spagnolie and P. T. Underhill. Swimming in complex fluids. *Annual Review of Condensed Matter Physics*, 14:381–415, 2023.

I. W. Stewart. *The static and dynamic continuum theory of liquid crystals: a mathematical introduction*. Crc Press, 2019.

J. Sznitman and P. E. Arratia. Locomotion through complex fluids: an experimental view. In *Complex Fluids in Biological Systems*, pages 245–281. Springer, 2014.

S. Wang and A. M. Ardekani. Unsteady swimming of small organisms. *Journal of Fluid Mechanics*, 702:286–297, 2012.

S. Weady, D. B. Stein, and M. J. Shelley. Thermodynamically consistent coarse-graining of polar active fluids. *Physical Review Fluids*, 7(6):063301, 2022.

K. Yeo, E. Lushi, and P. M. Vlahovska. Collective dynamics in a binary mixture of hydrodynamically coupled microrotors. *Physical Review Letters*, 114(18):188301, 2015.

B. J. Yoon and S. Kim. Note on the direct calculation of mobility functions for two equal-sized spheres in Stokes flow. *Journal of Fluid Mechanics*, 185:437–446, 1987.

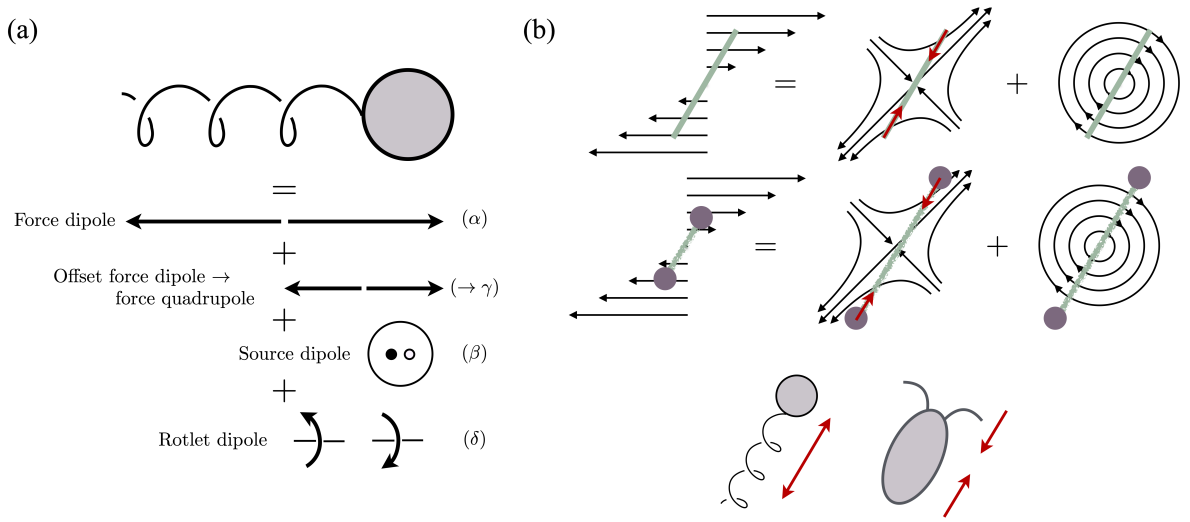

Figure 2: (a) The disturbance flow due to a swimming *E. coli* cell, envisioned as a multipole expansion. The leading order disturbance flow for a neutrally buoyant microorganism is a stresslet, carrying only information about whether the body is extensile or contractile (this coefficient can be time-dependent). Other geometric details enter at higher order in the inverse distance. Reproduced from Spagnolie and Lauga (2012). (b) Rods resisting extension (top), dumbbells resisting stretching (center), and force/torque-free active particles (bottom), all contribute a stresslet at leading order in the inverse distance (r^{-2} in three dimensions).

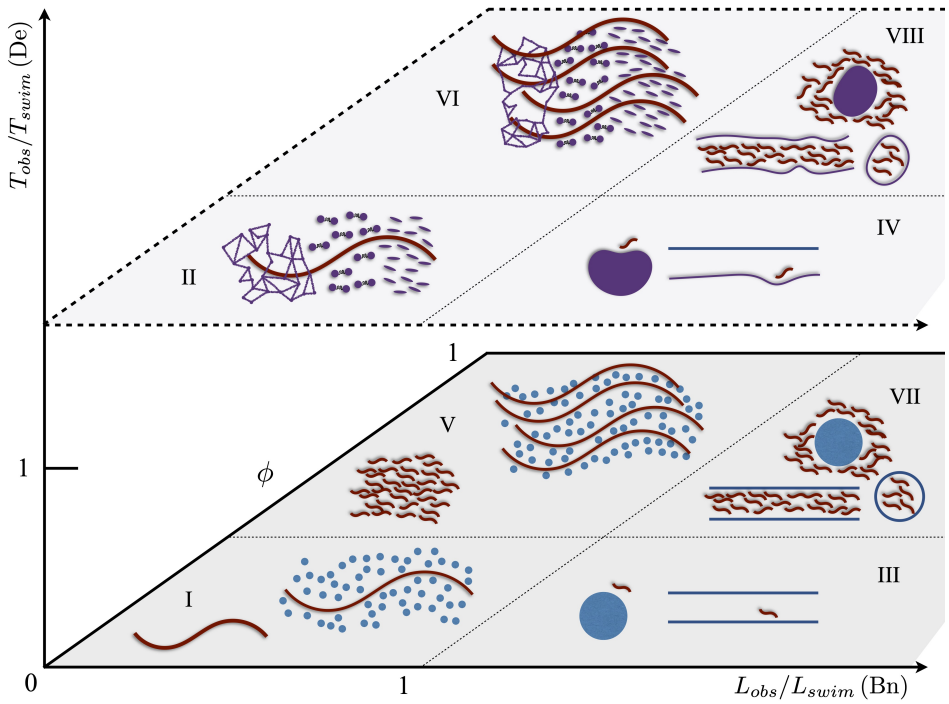

Figure 3: A classification of bodies immersed in complex fluids, organized along three axes: the size of the obstacles relative to the swimmer, $\mathrm{Bn} = L_{\mathrm{obs}}/L_{\mathrm{swim}}$; the relaxation time of the medium relative to the flow, the Deborah number $\mathrm{De} = T_{\mathrm{obs}}/T_{\mathrm{swim}}$; and the volume fraction of swimmers ϕ. The eight labelled corners are limiting regimes ranging from a single swimmer in a Newtonian fluid (I) to dense active suspensions in viscoelastic/structured media (VIII). Reproduced from Spagnolie and Underhill (2023).

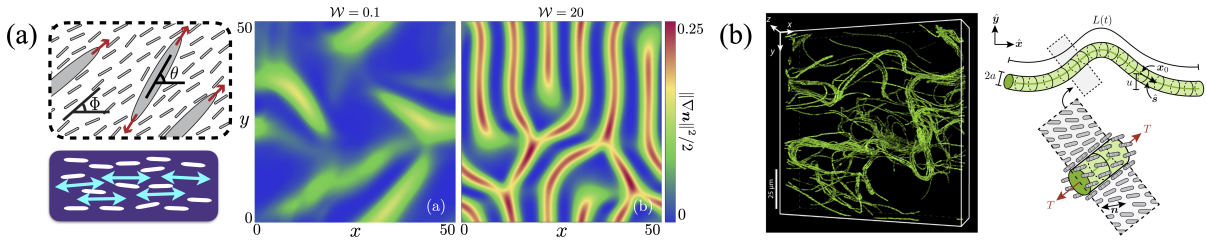

Figure 4: Examples of active matter in complex fluids. (a) A suspension of active particles immersed in a background nematic LC. Chaotic dynamics at small anchoring strength gives way to a steady, arrested flowing state at large anchoring strengths. Color indicates the degree of elastic energy stored locally in the LC. Reproduced from Li et al. (2025). (b) Growing and dividing immotile *E. coli* cells in a nematic LC, which resists bending. The colony remains elongated and is stable to transverse perturbations, leading to giant bacterial chains 200 times longer than an individual cell. Beyond a critical length, the chain buckles. Reproduced from Gonzalez La Corte et al. (2025).